Lake level changes and paleo-precipitation estimations based on stratigraphy of Holocene sediments in West Anatolia (Simav Graben)

Catherine Kuzucuoğlu, Faruk Ocakoğlu, Aydin Akbulut, Çiler Çilingiroğlu

Palaeogeography, Palaeoclimatology, Palaeoecology 597 (2022) 111001

Contents lists available at ScienceDirect

Palaeogeography, Palaeoclimatology, Palaeoecology

journal homepage: www.elsevier.com/locate/palaeo

Lake level changes and paleo-precipitation estimations based on colluvial stratigraphy of Holocene sediments in West Anatolia (Simav Graben)

Faruk Ocakoğlu [a,*], Catherine Kuzucuoğlu [b], Aydın Akbulut [c], Çiler Çilingiroğlu [d]

[a] Eskişehir Osmangazi University, Department of Geological Engineering, 26480 Eskişehir, Turkey
[b] Laboratoire de Géographie Physique, CNRS, UMR 8591, 92195 Meudon Cedex, France
[c] Hacettepe University, Department of Environmental Engineering, 06800 Ankara, Turkey
[d] Ege University, Faculty of Letters, Protohistory and Near Eastern Archaeology Department, 35100 İzmir, Turkey

ARTICLE INFO

Editor: Paul Hesse

Keywords:
Sediment facies analyses
Hydrological balance model
Quantitative precipitation data
Drought events
Holocene
Western Anatolia

ABSTRACT

Time-controlled quantitative climate data are crucial for reconstructing past environmental contexts of human history. In west Anatolia, the Simav Graben used to be occupied by a lake. However, today it is drained and associated with Holocene sediments that record lake level changes. An initial drill-core at the lake's centre reveals an arid phase before ca. 14 ka (i.e. prior to the Late Glacial warming) followed by a wet phase (marshes and lake) throughout the Holocene. Along the lake's margin, two additional sediment sequences contain a detailed Holocene record of changes in humidity throughout the Simav Graben's watershed. Classification of the shoreline facies from these sequences records drought events marked by colluvium prograding towards the lake. Using 13 radiocarbon dates, sedimentary facies suggest rapid lake contraction phases grossly around 8.0, 3.9, 2.9, 2.4 and 2.0 ka. After the drier periods, recorded by phases of terrestrial progradation, lake level increase is marked by retrogradational lake muds and peats onlapping the colluvium, consistent with increases in total lake volume. Based on modern lake morphology, climate and runoff data, and the elevations recorded by the shoreline facies identified within the marginal Holocene sedimentary sequence, we constructed a paleohydrologic balance model and a precipitation curve. According to the model, annual precipitation may have been fallen below 460 mm during the 8.2 ka event, and 468–478 mm during the 4.2 ka and 3.2 ka events – demonstrating an extreme decrease in precipitation compared to the earlier wet phases. In turn, Holocene Archaeology in West Anatolia outlines (i) a widespread abandonment and/or notable fire events at the end of the Early Bronze Age III (ca. 4.2 ka), and (ii) a high level of social instability at the beginning of the Early Iron Age (ca. 3.2 ka). The correlation between the timing of lake level falls at Simav (water volume depletion caused by drying trends) at 8.0 ka, 3.9 ka and 2.8 ka and cultural fluctuations suggest that drought events may have played a major role in these socio-political changes in western Anatolia. Furthermore, the high lake-level stages (associated with precipitation >500 mm) coincide with the Late Chalcolithic to Early Bronze *Age* I transition as well as the Hellenistic and Roman periods, both times of economic stability and growth in the region.

1. Introduction

Paleoclimatology is the study of climate dynamics before the implementation of modern instrumentation. In some geological archives, such as varved ice and lake deposits, time can be resolved to produce yearly to decadal records of past climate change (Jones et al., 2009). Furthermore, the understanding of past climates and their impact on human ecology during the Holocene is important in order to forecast the threat to Earth's biosphere due to the ongoing global warming, which demonstrates the importance of obtaining such absolute past climate parameters on the local to regional scales, which can be extrapolated globally (Kohfeld and Harrison, 2000; Roberts et al., 2018; Finné et al., 2019). This latter approach applied to lake levels (associated with water budgets in the watershed), needs to first be calibrated to modern datasets that include recent meteorological parameters, before paleodata can be interpreted in terms of past climates (Hastenrath and Kutzbach, 1983; Pribyl and Shuman, 2014; Morrill et al., 2019).

Holocene climate shifts towards drier conditions are generally characterised by a decrease in precipitation and temperature, an increase in the frequency and magnitude of temperature and precipitation

* Corresponding author.
E-mail address: focak@ogu.edu.tr (F. Ocakoğlu).

https://doi.org/10.1016/j.palaeo.2022.111001
Received 9 September 2021; Received in revised form 6 April 2022; Accepted 12 April 2022
Available online 19 April 2022
0031-0182/

events, and ultimately a negative shift in the water budget (Mayewski et al., 2004; Reyer et al., 2017; Hoegh-Guldberg et al., 2018). This conceptual model is generally accompanied by sparse vegetation cover and its compositional change (Morecroft and Keith, 2009; Dormoy et al., 2009). Here, we also consider the impact of human activities with regards to sediment dynamics by land-use change at different scales, which might be irrelevant to climate (Kaniewski et al., 2007; Dusar et al., 2012). Recent studies outline that the impact of human activities in the Eastern Mediterranean became the prime driver on sediment dynamics in the late Holocene (in archaeological terms "Bronze Age"), and accelerated particularly in dry periods (Dusar et al., 2011, 2012). However, tree cultivation data from the entire northern Mediterranean region demonstrate human impact on land cover occurred much later (after 3500 yr B.P.) (Roberts et al., 2019). Conceptually, we expect a direct impact of these drivers on the stratigraphic record of lake margins. Presently, there is no efficient way to connect changes in the stratigraphic record to past human activities as detailed local archaeological investigations in the Simav area are scarce. Nevertheless, the paleoclimatological proxies including the past water budget studies, and their correlation with other paleoclimatological records elsewhere can provide some insights regarding the impact of climate upon sediment dynamics.

Inland closed lakes are very sensitive to climate changes and provide rich opportunities to paleoclimatologists. Nevertheless, most of the proxy records from lakes provide only a picture of relative climate changes of the past, which strongly restricts how we understand the responses of past societies to these changes. Many regional-to-global drought events in the Holocene should have resulted in the shrinkage or desiccation of inland lakes, which should also be recorded in biological and chemical/isotopic proxy data in lake sediments. As a result, the detrital systems (i.e. alluvial and colluvial fans) around lakes indicate progradation during dry periods. However, the increase in human activities alone can also accelerate the sediment dynamics that have been clearly shown throughout the eastern Mediterranean. Therefore, a combined effort that integrates the multi-disciplinary study of marginal and central sediments of lakes to the current hydrological data are needed to construct a paleohydro-balance model, which enables the estimation of quantitative precipitation data for the past drought events. Moreover, the correlation of these events with other well-dated high-resolution climate records elsewhere can provide some insights into the relative significance of the involved drivers.

This study investigates a lakeside colluvial wedge using paleoclimatological proxies in Lake Simav (W Anatolia) which was drained and dried out in 1959. This lakeside record is particularly valuable because it enables quantitative precipitation estimations for many archaeologically significant timelines. Although the quantitative approach to paleoclimatology is rapidly advancing worldwide, it is still limited in the Anatolian Peninsula where integrated isotope-hydrology models, pollen and tree-ring based precipitation estimates, and cladoceran and diatom based salinity reconstructions are rare (Jones and Mann, 2004; Jones et al., 2007; Touchan et al., 2007; Woodbridge and Roberts, 2011; Çakıroğlu et al., 2016). More specifically, the present study aims to 1) describe and date Holocene lakeside colluvium within the stratigraphic record and discuss their paleoclimatological implications, 2) correlate dry periods of the Simav area with regional drying trends evidenced elsewhere, 3) determine past annual precipitation trends using a hydro-balance model of the lake, 4) compare the past quantitative precipitation values and trends with other paleoenvironmental and paleoclimatic records in the Eastern Mediterranean, and 5) discuss their historical implications.

2. Hydro-balance models

A hydro-balance model considers the balance between the three parameters in a hydrologically closed basin (Hastenrath and Kutzbach, 1983).

$$P = E_w a_w + E_l (1 - a_w) \quad (1)$$

where P is the basin average precipitation, $E_w a_w$ is the evaporation from the lake surface, and E_l (1 - a_w) is the evaporation from the land surface, including plant respiration. If the amount of outflow (or leakage) is known, this equation can still be applicable in open systems by adding the latter to the right of the formula.

In practice, the most challenging parameter of this equation is quantifying the evaporation from the land surface, which is closely related to vegetation cover and ground characteristics (Hastenrath and Kutzbach, 1983; Grillone et al., 2014). An important derivative of this parameter is the surface runoff, described as the proportion of precipitation remaining after infiltration and evaporation on the land surface. This term is frequently determined empirically due to the complications of the input model parameters (i.e. slope, geology, soil type, vegetation, climate parameters) (Grillone et al., 2014). Therefore, if the surface runoff rate is known, precipitation can be calculated for a given lake when the bathymetry and lake level are available.

Evaporation from the lake surface essentially varies with the ambient temperature in a given area. As pollen-based estimations demonstrated, the mean annual temperature in SE Europe including Anatolia dropped ca. 0.5 °C in Middle-Late Holocene and up to 1.5 °C in early Holocene during the Rapid Climate Change (RCC) events (Davis et al., 2003; Dormoy et al., 2009). For this reason, the impact of this temperature deviation on evaporation from the lake surface should also be considered. The estimated rate of 1 °C drop on evaporation is 7.2% for Australian lakes over the course of global warming (Helfer et al., 2012), 6.0% for a Romanian lake (Stan et al., 2016), and 6.3% for the Simav area (Table S1).

The potential of the hydro-balance model has been demonstrated in many studies. For instance, Hastenrath and Kutzbach (1983) used a hydro-balance model to show that the P was 150–300 mm higher (15–35%) between 7 and 10 ka when higher lake levels prevailed in Lake Turkana. Junginger and Trauth (2013) successfully determined P and T in the North Kenyan Rift during the African Humid Period (5–15 ka). In another example, DeVogel et al. (2004) estimated past precipitation conditions using a GIS-based reconstruction of late Pleistocene terraces of known age in central Australia. Finally, the hydro-balance model has been used to reconstruct the water budget of Lake Van in eastern Turkey using the late Pleistocene terraces (Christol et al., 2010; Kuzucuoğlu et al., 2010).

In this study, in addition to a proxy-based paleoclimatological investigation, we also applied a hydro-balance model to estimate past precipitation in the Lake Simav watershed using modern run-off data and past lake levels.

3. Study area

3.1. Geological and geomorphological outline

The Simav Graben is one of the depressions controlled by the NW-SE striking Akşehir-Simav Fault System in the West Anatolian Extensional Province (Koçyiğit and Deveci, 2005). Two morphologically distinct *E*-W striking control faults delimit the depression in the south and north, while the shorter fault segments connect them to each other in the east (Fig. 1A). There is multiple seismological, geomorphological, and geothermal evidence for the current activity of these basin margin faults (Emre and Duman, 2011; Özden et al., 2012). Conversely, the flat and structureless graben floor does not manifest any evidence of faulting such as linear ridges or sags and seems to subside passively in response to marginal faulting events. It is probable that past large (Mw > 7) faulting events at basin margins would have induced lake level changes due to tilting of the graben floor, but their impact on the lake level may have been limited (<10 cm) based on the tilting in comparable seismic events elsewhere (Meschis et al., 2019). Highlands surrounding the lake

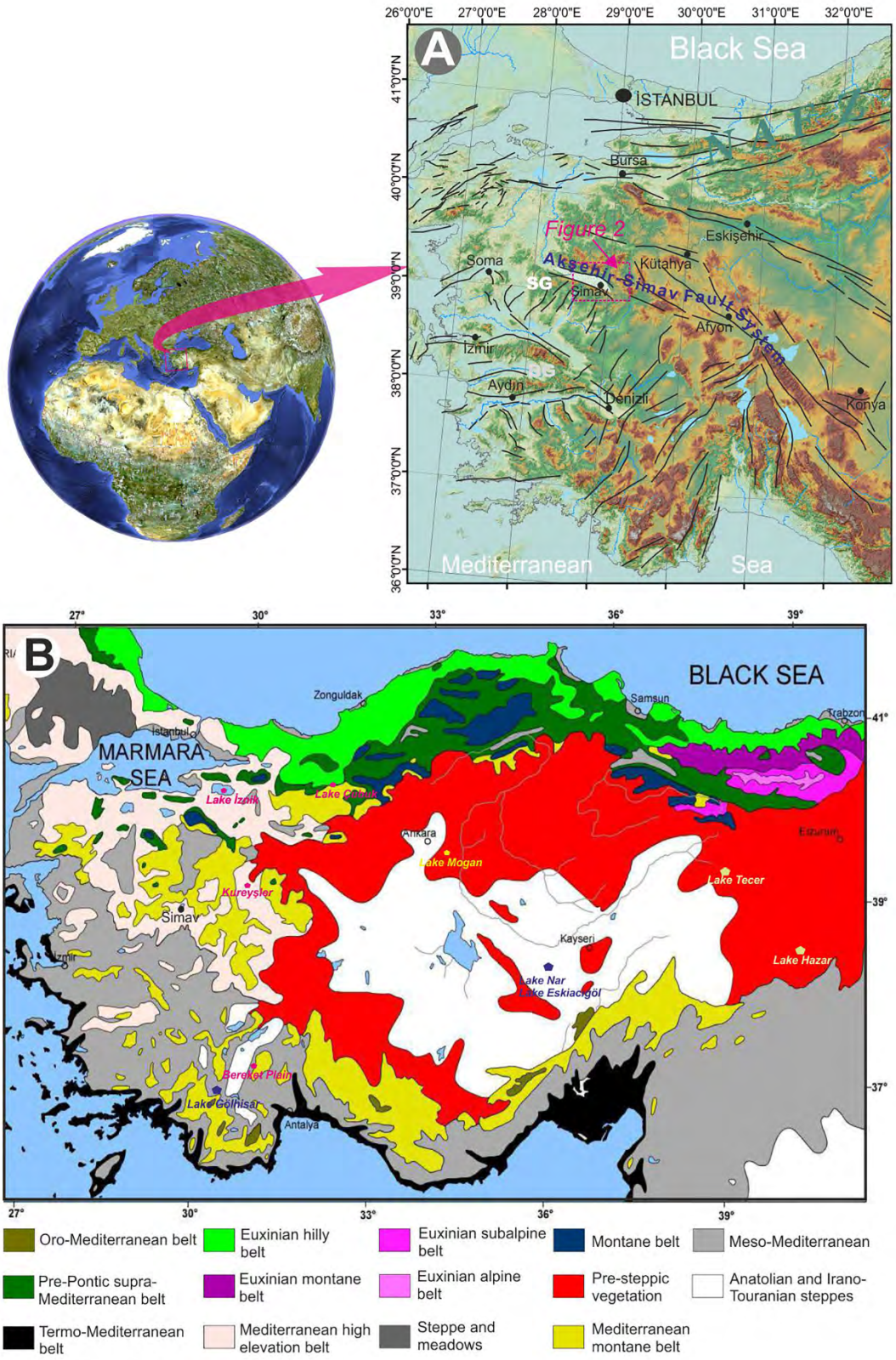

Fig. 1. The physical context of western Anatolia.
A: Morphology and active tectonic outlines. Compiled from Bozkurt (2001) and Yaltırak (2002). SG = Simav Graben.
B: Vegetation Zones. Based on Quezel and Barbero (1985).

basin consist of Paleozoic eclogites and marbles in the south and of Oligocene-to-Miocene terrestrial sediments and magmatic rocks in the north (MTA, 2002). Erosion of the highest landscape in the south and the east of the depression feeds alluvial fans formed of coarse materials (Fig. 2). Some of the alluvial fans (in the vicinity of Yeşilyurt, E of Çitgöl and Güneyköy villages) are so large that they alter the configuration of the basin floor. In the middle of the graben, an inherited N-S trending basement bench has divided the basin into two parts (Ocakoğlu et al., 2019a) which are connected by the Simav Creek that incises the fluvial infill in the basin's western segment (Fig. 2). The basin is also characterised by a thick sediment fill in the eastern segment. Elevation of the marginal basin floor is about 790–830 m above sea level (asl) (the southern highs reaching >1500 m asl above the graben floor) and 780 m asl when reaching the *E*-W central axis of the graben. The basin fill which is composed of >400 m thick lacustrine mud was drilled by the State Hydraulic Works (DSİ) (Eser, 1997; Ocakoğlu et al., 2019a). The centre of this graben was occupied by a widespread wetland (shallow lake and marshes) until the end of the 1950s when the lake dried after a former outlet channel north of Boğazköy village was deepened down to 2–3 m below the lake bottom. This drainage aimed at transforming the lake floor into agricultural fields. According to Sicim (2010) and Bingöl and Korkmaz (2013), the desiccation process went on for 20 years until 1980. Today, the channel is still not wide enough to prevent the accumulation of water in the rainy winter and spring seasons.

There are three gorges that could have served as outlets to Lake Simav in the past. The Ortaboğaz Gorge to the north (Fig. 2) stands at 785 m asl at the southernmost end of the north-flowing Mustafa Kemal Valley. The Savcılar Gorge is situated at 794 m asl along with the skirts of the southernmost alluvial fans sourced from the northern basin margin. The final potential exit is the gorge of Boğazköy which was deepened over 6 m in the metamorphic basement as the lake was drained in 1959 (Figs. 3A, 4A, B). According to local villagers, the lake level was 784 m asl at that time, corresponding to a discernable sandy/silty shore near the village of Boğazköy (Fig. 3A). Assuming a constant sedimentation rate along the alluvium-filled Savcılar and Ortaboğaz gorges through time, these data indicate that Lake Simav was an endorheic basin when the lake depth dropped below 4 m.

3.2. Climate setting and vegetation cover

In the Simav area, annual data define a mild and humid Mediterranean-type climate where summer months are dry and warm. In detail, the study area belongs to the transitional "Marmara Climate", which extends between the Black Sea and Mediterranean Sea (Ünal et al., 2003). Despite high annual precipitation (814 mm y^{-1}) in this climate region, seasonality is prominent such that the area is classified as semi-arid to poorly humid according to the Thornwaite Classification scheme (Meteoroloji Genel Müdürlüğü, 2020). However, the Simav area is one of the least arid localities in the climate region according to various aridity indices all over the country except in the Black Sea Region (Şahin, 2012). The meteorological files between 1938 and 2010 from the Simav Station reveal that almost half of all rainfall occurs in the winter months, while the summer months receive only 7% of the total (Table S2; Meteoroloji Genel Müdürlüğü, 2020). The mean annual temperature stands at 11.8 °C while that of the summer months is over 20 °C (Saldık, 2019). Accordingly, the potential annual evaporation (866 mm) exceeds the rainfall – particularly from April to September.

The present climate of the study area is controlled by the North

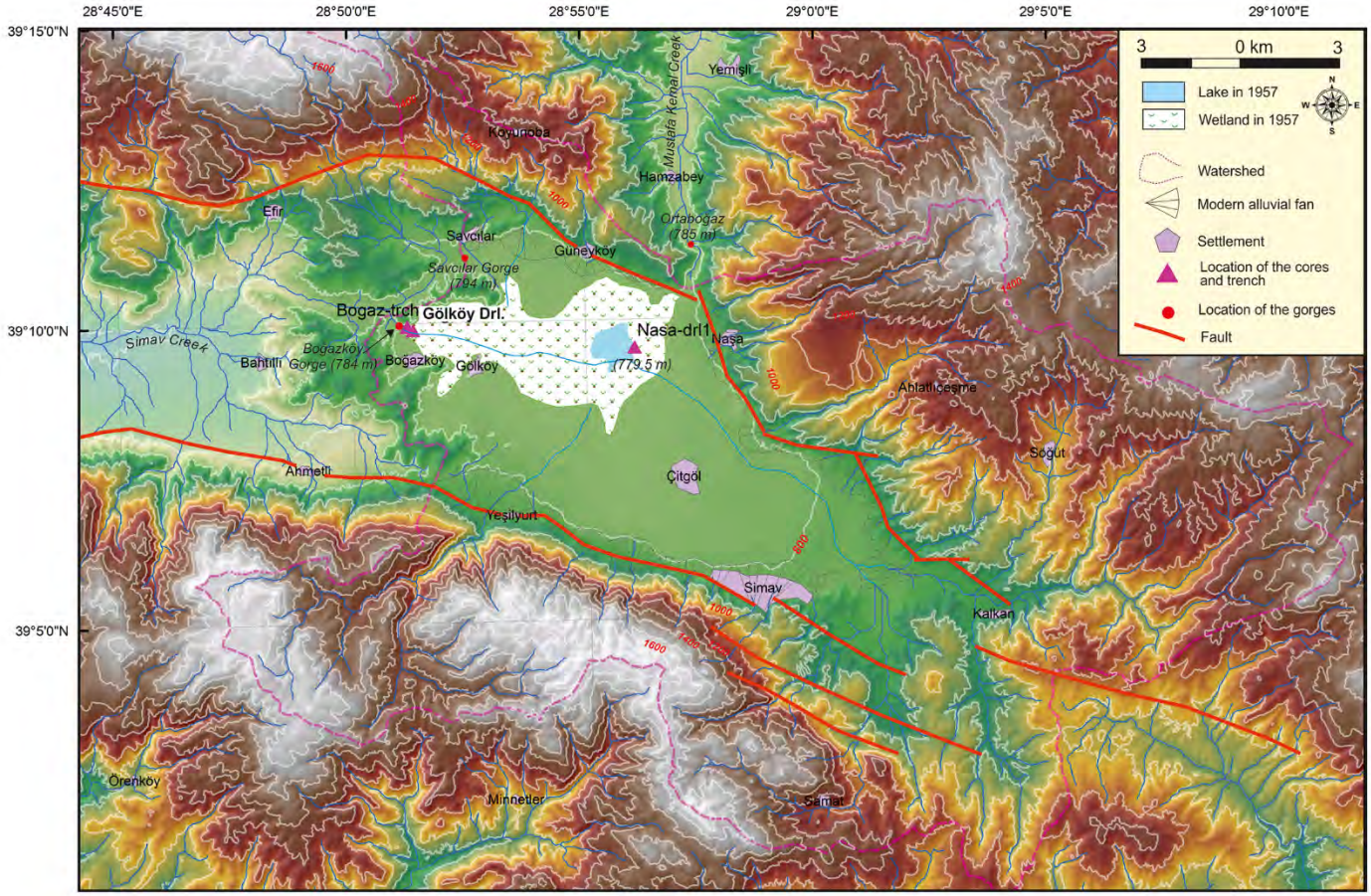

Fig. 2. Morphology of the Simav Graben with location of sections and cores studied (Boğaz trch: Boğazköy Trench, Gölköy drl: Gölköy Drillhole, Naşa drl1: Naşa Drillhole).

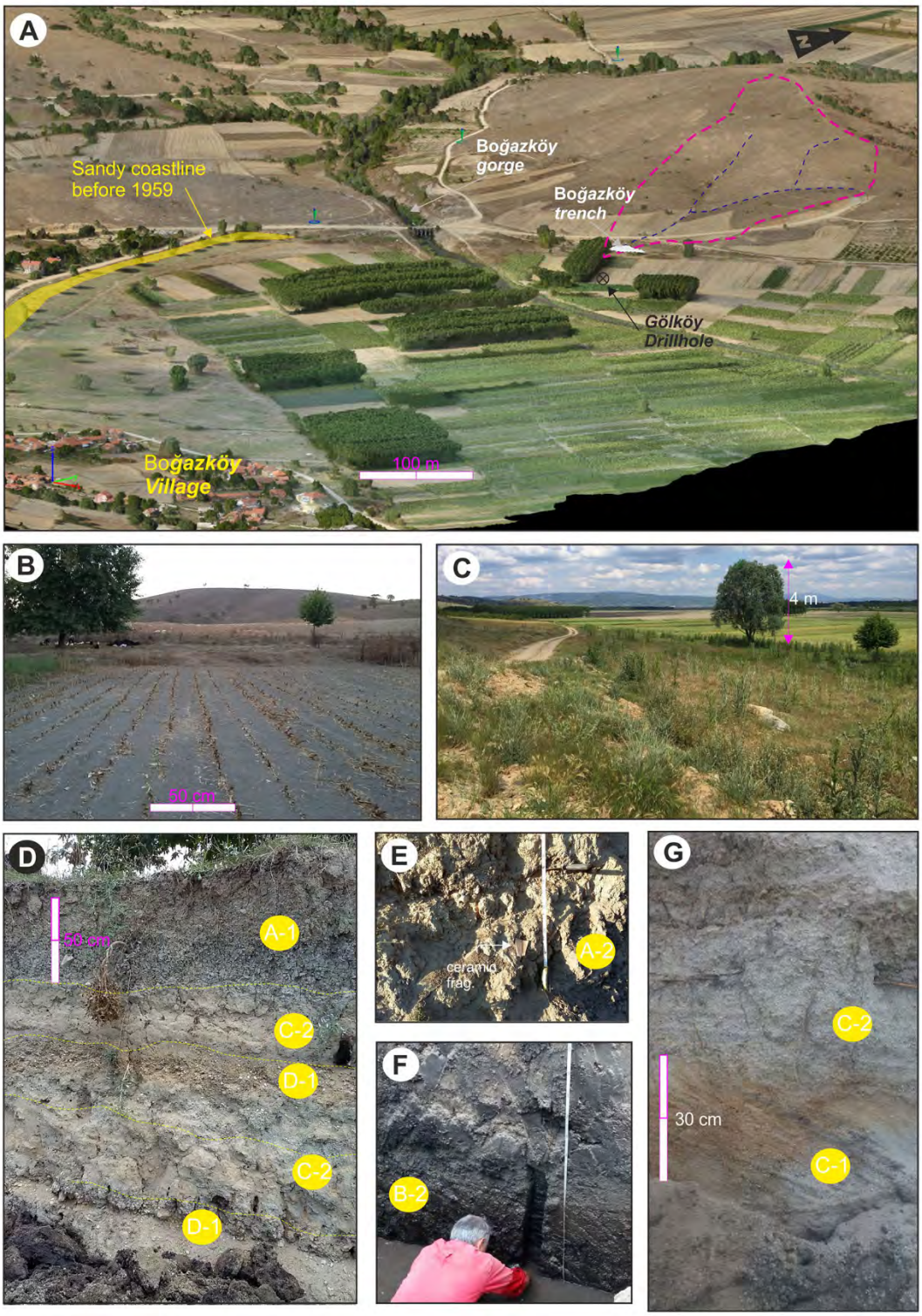

Fig. 3. Field views around the main area studied (upslope the present outlet).
A: UAV view of the western limit of the paleo-Simav Lake where the Boğazköy section was entrenched.
B: View of the small watershed above the Boğazköy Trench. Note the recent grey lake muds blanketing the ground, which covered the lake floor before the present artificial outlet started to operate.
C: View of the colluvial wedge inclined westward in direction of the paleo-lake floor.
D: Alternating muddy and sandy facies in the trench section. Yellow circles denote different facies (see Fig. 5A and text for facies explanation).
E: Lacustrine facies containing ceramic fragments (upper part of the trench).
F: Sampling of the peat deposits forming the lower part of the trench.
G: Well-sorted coarse sand clinoforms overlying flat sands in the trench section. (For interpretation of the references to colour in this figure legend, the reader is referred to the web version of this article.)

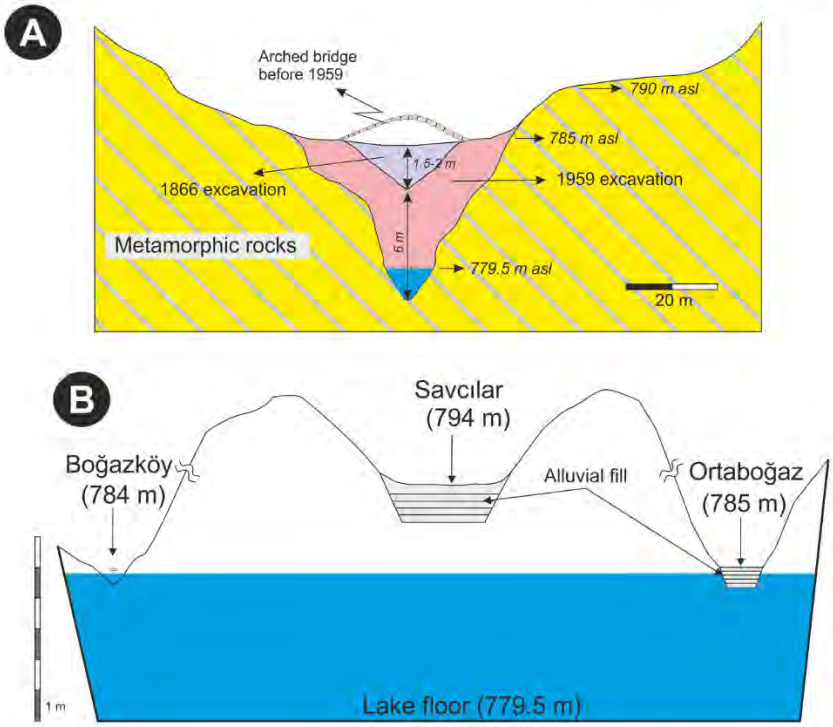

Fig. 4. A: Human-made incisions of the Boğazköy Gorge during the Late Ottoman period and the Turkish Republic. Elevation of the arched bridge and the thalweg before 1959 CE is based on anecdotal information from the local people and confirmed by the shoreline evidence in Fig. 3A. B: Schematic cross-section showing elevation of three outlets and the floor of the Simav Graben.

Atlantic Oscillation (NAO) (Lionello et al., 2004), a weather phenomenon that is a result of spatially and temporally contrasting high- and low-pressure systems over the North Atlantic Ocean. The NAO controls the westerly winds and storm tracks across the North Atlantic Ocean, through western Europe and the Balkans, and also influences western Anatolia's inland climate (Lionello et al., 2004). However, abundant winter precipitation triggered by the NAO diminishes eastwards over Anatolia (Türkeş and Erlat, 2003; Küçük et al., 2009). Similarly, the Azore high-pressure system transports warm and humid Atlantic air masses eastwards. However, the Azore high-pressure system loses its humidity as it moves towards the Aegean Sea, which brings hot and dry air to the Anatolian western coast. During winter, the Siberian High (another high- and low-contrasted pressure system centered around the northern Pole and northern latitudes) generates cold and dry winters over Anatolia (Tatlı et al., 2004; Sariş et al., 2010). In this light, the Anatolian climate is complex, and knowledge of the teleconnections between the different climate modes is significant, especially when trying to understand the dynamics and drivers of the Holocene climatic changes (Lionello et al., 2004; Küçük et al., 2009).

Vegetation cover in the Simav area is dominated by deciduous flora belonging to the Supra-Mediterranean mountain belt at higher elevations (Fig. 1B; Quezel and Barbero, 1985). The north-facing steep slopes are host to a dense *Pinus nigra* population. More sheltered, humid parts of these slopes are covered with moisture-demanding species such as *Fagus*, *Alnus glutinosa*, *Corylus avellana* and *Tilia* (Sicim, 2010). The centre of the graben hosts wetland vegetation such as *Phragmites australis,* and *Typha* sp. – especially abundant along drainage channels. The northern and eastern parts of the graben are covered by degraded forests consisting of *Pinus brutia*, *Juniperus oxycedrus*, *Quercus coccifera*, frequently interrupted by cleared fields, consisting of bean, corn and sunflower (Recep, 1998). In summary, the former lake floor is currently devoted to agricultural production while its margins are covered with degraded forest and cultivated trees.

4. Methodology

The Holocene stratigraphy of the study area is based on a trenched section (Boğazköy Trench) along the western margin and two drill holes. One drill hole (Gölköy Core) is near the Boğazköy Trench, whereas the other drill hole (Naşa Core) was taken at the centre of the dried lake (Fig. 2). One additional core (Naşa Livingstone core) for cross-check purposes was drilled very close to the Naşa Core.

The Boğazköy Trench was dug with an excavator in two phases. The first phase consisted of drilling down 300 cm from the floor of the coastal landform at 783 m asl. In the second phase, the excavator cut a second trench within the floor reached in the first phase down to 520 cm where the underground water table was reached. The third and final phase consisted of drilling with a Livingstone corer to sample a further 160 cm down. Sampling over the upper 500 cm sections was performed every 5 cm, while sampling in the cores was performed every 3 cm.

The Naşa and Gölköy cores were retrieved using a traditional truck-mounted drilling machine. The Naşa drill hole reached a depth 18 m below the ground surface at 779.5 m asl. Here, we only present the upper 9 m that correspond to the Holocene deposits specific to the present study. Additionally, we did shallow (4.2 m) supplementary Livingstone coring (*Naşa Livingstone core*) in order to double-check the original core. The Gölköy drill also reached 9 m depth from the ground surface at 780 m asl. Based on the drill cores' equal surface elevation and depths, we show the deposits are comparable in both drill cores. In the article, only the lithology and age profiles of the Naşa and Gölköy cores are presented. Presently, five different proxies have been implemented in the Boğazköy Trench section:

(1) Magnetic susceptibility (MS) measurements were performed on the mass-specific base (1% precision) using a Bartington MS2B laboratory sensor on dried and powdered samples (Table S9).

(2 and 3) LOI_{550} and LOI_{950} values which are indicators of total organic carbon (TOC), to compare with the total carbonate content (TCO_3) were determined by loss on ignition tests (4 h heating 3 g sample weight at 550 °C for TOC, and further 2 h heating at 950 °C for TCO_3)

(see the procedure in Santisteban et al., 2004). The equations, $T_{CO3} = 1.36*LOI_{950}$ and $T_{OC} = LOI_{550}/2$ by Heiri et al. (2001), are applied for the transformation of loss on ignition results to total carbonate and organic matter contents respectively (Table S9).

(4 and 5) Stable isotopes of C from the organic fraction ($\delta^{13}C_{org}$) and $\delta^{15}N$ from the bulk sediment were measured using the Elemental Analyser-Isotope Ratio Mass Spectrometry (EA-IRMS) technique in Iso-Analytical Laboratory (UK). The procedure, reference materials and quality control issues are explained in Table S8, and the results are given in Table S9.

(6) Diatom analysis was conducted using the pollen slice preparation method by Round et al. (1990). 600 diatom frustules were counted in each slide following Battarbee (1986). Here we only consider the ratio of benthonic to planktonic diatom species (Table S9). Species-based diatom abundance, as well as their paleoenvironmental significance in the Boğazköy Trench section, was given in detail elsewhere (Ocakoğlu et al., 2019a).

(7) All the geochronology in this study were done using the AMS Radiocarbon technique in Beta Analytical (UK), Georgia University (USA) and ARTEMIS Laboratory (Saclay Univ., CEA/CNRS). Radiocarbon ages were calibrated using CalibRev. 8.2.0 software following the Intcal20 database (Stuiver et al., 2021) and expressed as 1 sigma mean ages. Age-depth and sediment accumulation rate models of the Boğazköy Trench section were prepared using Bchron R software (Haslett and Parnell, 2008; Parnell et al., 2008).

The hydro-balance model in this study considers the equality of water input and output in a closed lake system to sustain the lake level constant following the equation below:

$$P_{ann} x D_a x RC = L_a x E_m x (1–0.07 x \Delta T) \quad (2)$$

where P_{ann}: Annual precipitation, RC: runoff coefficient, D_a: total drainage area, L_a: Lake area, E_m: modern evaporation, and ΔT is the temperature decline of the mean warmest month (MWAM) during the RCC events compared to modern. In this study, the meteorological data used (monthly precipitation and evaporation) belong to the Simav Meteorological Station (Devlet, 2020). The runoff data between 1979 and 1993 were also measured by the same institution at the Boğazköy Gorge which constitutes the only outlet of the basin in modern times. Lastly, the ΔT values were taken from the SE European pollen-based temperature dataset including Anatolia (Fig. 3 in Davis et al. (2003)).

If the surface area and volume of a lake are known for a timeline, the right of the equation (i.e. output or the total evaporation from lake surface) can be calculated. This volume equals the annual runoff into the lake. The surface area and volume of the lake are calculated in turn using two other datasets. 1- The past lake level: This is the elevation of the past coastline that was identified by sedimentological observations in the Boğazköy Trench Section 2. The past bathymetry of the lake: This is reconstructed by the extraction (also called backstripping) of a sediment thickness, the base of which corresponds to the target timeline in the lake centre (Naşa) core, from the current topography using ArcGIS 10 software. Here, the elevations of the top of the Trench section and Naşa core were measured using a cm-precision dGPS device. The graben floor's ALOS elevation data with 15 m horizontal resolution were rectified using ground control points of dGPS measurements (ALOS PALSAR, 2020). Then, these lake level and bathymetry data are appended to calculate the volume and area of the lake for a given lake level using the *Surface Volume* script under *3D Analyst* module in the same software. Throughout our calculations, compaction was ignored due to the thin and water-saturated nature of the studied lake sediments.

The next step in the hydro-balance model is the estimation of runoff coefficient (RC) for different climatic conditions. For this purpose, we analysed the modern hydrological dataset (Table S1-S6) and produced an exponential relation ($RC = 0.2244\ln(P_{ann})-1.3078$) between RC and P_{ann}. Lastly, we empirically determined the P_{ann} that satisfies the volume of evaporation from the lake surface in Eq. (2) above. Here, the applicability of runoff coefficient to the past with unknown vegetation cover can be questioned. Nevertheless, the unpublished pollen data in Naşa core (Ocakoğlu et al., 2019a) reveal consistent abundance of herb pollen around 5% (modern values: 2–3%) throughout Holocene (though rare spikes up to 10–15% also occur) suggest the reliability of the model.

5. Results and interpretation

5.1. Data from the trench and the cores

5.1.1. Boğazköy trench

The Boğazköy Trench (39° 09′ 52" N, 28° 51′ 09″ E) was dug on a gentle slope in the western margin of Lake Simav. The trench site is located on a colluvial fan sourced from a small (150 × 300 m) watershed within the basement schist and gneiss (Fig. 3A, B, C). The Boğazköy Gorge served as one of the outlets of the lake during the wet Holocene periods and is located just west of this colluvial fan. According to the available historical data, the gorge was deepened, first by the decree of Ahmet Vefik Pascha, a local governor of the Bursa Province, in 1866 likely to mitigate the flooding of lakeside villages (Simav Ticaret ve Sanayi Odası, 2020). A second and more radical deepening treatment that led to the complete desiccation of the lake occurred in 1959. Fig. 4A depicts the past and present elevations in the vicinity of the gorge as measured from a UAV-based topographic map.

5.1.1.1. Age-depth model. Seven out of 13 radiocarbon AMS charcoal analyses were used to establish the age model of the Boğazköy Trench section using the Bchron package (Parnell et al., 2008) (Fig. 5A; Table 2). Two of the remaining samples (Bog 672–675 and Bog 288) were tested for double-checking purposes of either the laboratory or the nearest sample and were found to be satisfactory. Three samples between 160 and 200 cm produced very close results confirming very high sedimentation rates. Therefore, the results of the samples Bog 200–202 and Bog 184–188 are not shown in Fig. 5A. Only one sample (Bog 509–512) displays complete contrast with the overall age model likely due to root penetration of young aquatic plants and is discarded.

According to the age model, the base of the trench record dates back to 8.2 ka whereas the uppermost lacustrine sediments correspond to 1950s A.D., i.e. just before the desiccation of the lake. No obvious time gap is detected in the model, but the curvature of the graph implies a variable sedimentation rate. The sediment accumulation rate (SAR) graph generated using the same software mentioned above shows relatively lower values before 4 ka (Fig. 5B). We suggest slightly higher rates in the lowest colluvium (COL-1) compared to subsequent lacustrine facies, especially after 5200 yr B.P. The first SAR pulse starts around 4100 yr B.P. and reaches the maximum in the second colluvial wedge (COL-2) (Fig. 5B). However, higher rates also apply to the overlying muds. Following a period of low accumulation rates in the lake facies, the highest accumulation rate occurs in the third colluvium (COL-3) at about 2800 yr B.P. Afterward, SAR values display a rapid stepwise decrease in the uppermost colluvium (COL-5) and the overlying muds (Fig. 5B).

5.1.1.2. Facies description. Five coarse-grained wedges interlayered with peat, dark organic matter-rich mud and grey mud occur in the trench section (Figs. 3D, 6A & 7). Herein, eight sedimentary facies each representing distinct depositional conditions have been identified. Short descriptions of the facies are given in Table 1.

As a brief aside, we note that of the sedimentary characteristics outlined here, the subaerial facies are characterised by almost lack of TOC and TCO_3 content while the aquatic facies are always finer-grained and contain abundant diatoms and reed remains.

5.1.1.3. Hydrodynamic and bathymetric interpretation of facies. Colluvial depositional systems are an undervalued branch of clastic

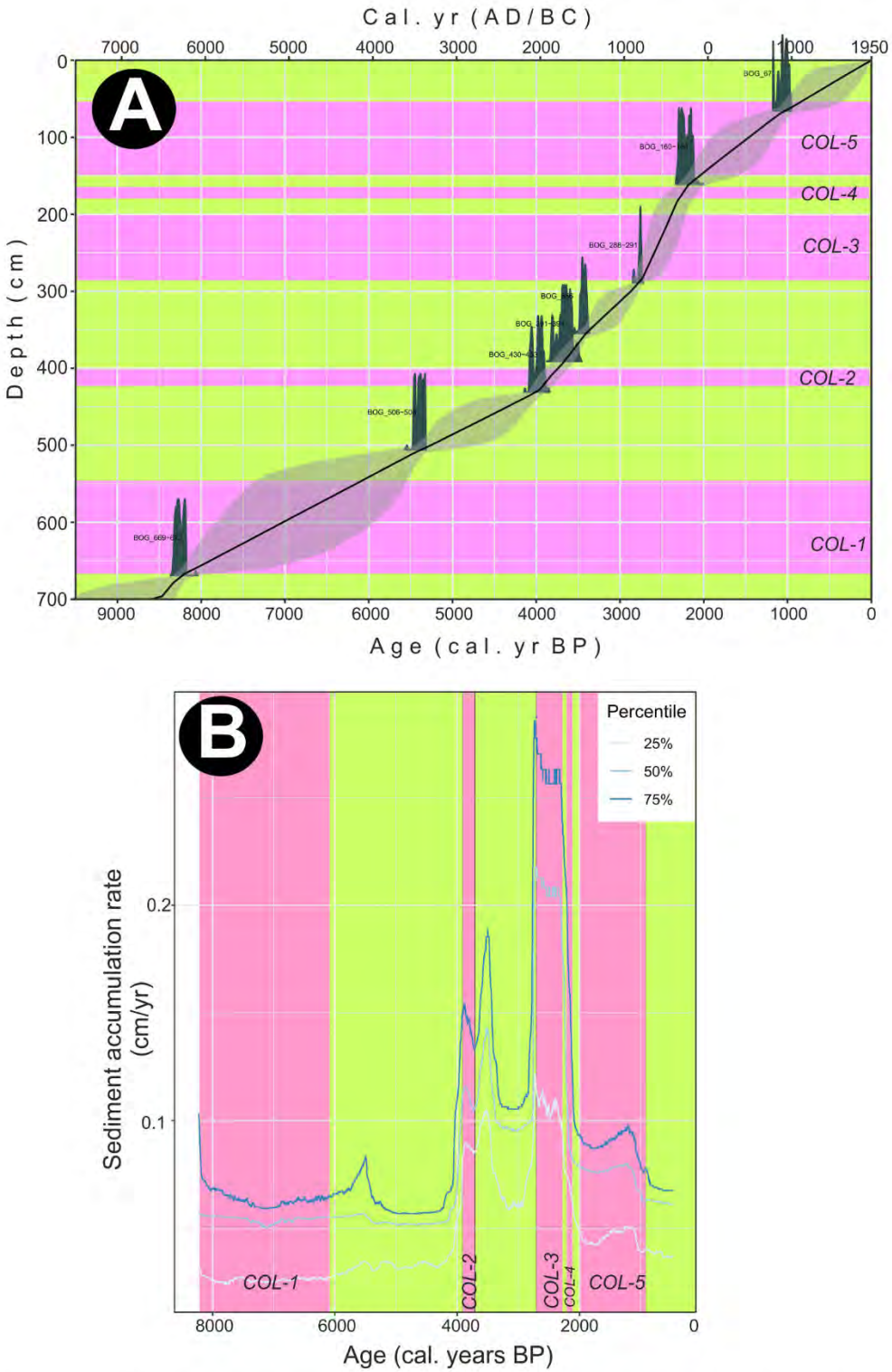

Fig. 5. A- Age-depth model B- Change of sediment accumulation rate (SAR) of the Boğazköy Trench section produced by the Bchron R software (Parnell et al., 2008). Pink and green bands represent colluvial and lacustrine facies respectively. See Table 1 for the full details of radiocarbon data. (For interpretation of the references to colour in this figure legend, the reader is referred to the web version of this article.)

sedimentology, despite being exceptional at recording paleoclimatic conditions (Brazier and Ballantyne, 1989; Blikra and Nemec, 1998). The apparent morphological framework and the facies types described in Table 1 confirm that the coarse-grained intercalations represent a colluvial system that episodically prograded into the Lake Simav. The massive gravel (D-1) and sandy gravel (D-2) facies most likely represent debris flow and subsequent fluid flow in the medial and distal parts of a colluvial fan respectively. Poorly-sorted coarser gravels with inter-granular sand facies (D-1) correspond to sieve deposits that form as a result of rapid vaining of fluid energy due to infiltration (Nemec and Kazancı, 1999). Towards distal part of the fan, a flow consisting of relatively finer-grained material turns into a sheet flow upon exiting

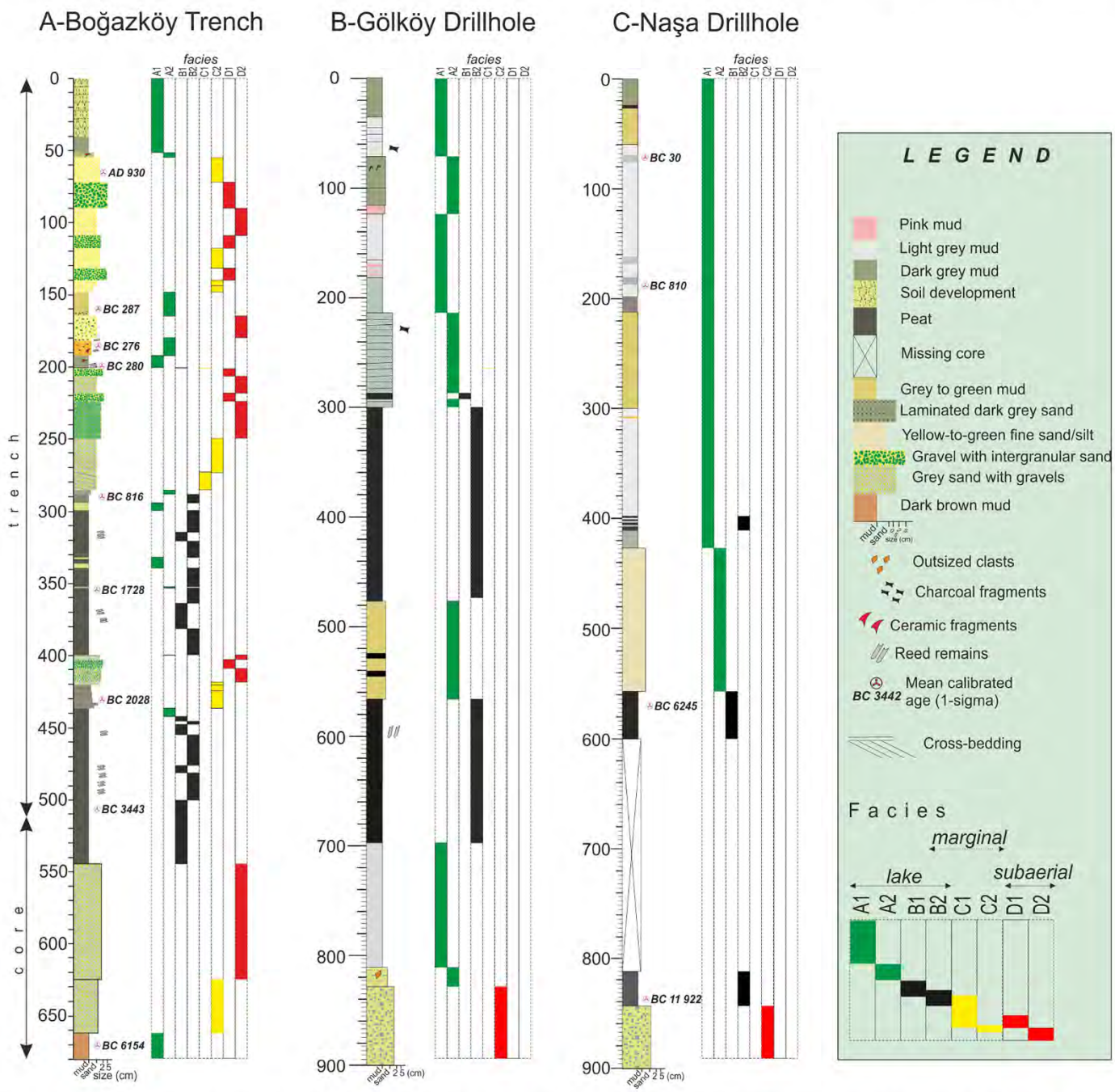

Fig. 6. Lithology and facies of sediment layers recording depositional changes in the Simav depression floor during the Holocene. Letters are for the location of the sequences.
A: Sequence from the trench section near the Boğazköy Gorge (trench section).
B: Sequence from the core (Gölköy Dirillhole) drilled in the graben floor close to the Boğazköy Gorge.
C: Sequence from the Naşa Drillhole.

confined portions of the fan. Furthermore, finer-grained gravels with crude bedding and mudflows associated with catastrophic precipitation can also occur. These processes explain the relatively finer-grained crude bedding and exotic gravels in Facies D-2. A stillstand or even fall of lake level result in progradation of the colluvial fan, which manifests as a change in the maximum clast size along with a vertical profile (Blikra and Nemec, 1998).

The sediments deposited along the lakeside become better sorted due to the removal of muddy sediments by wave action (Reineck and Singh, 1980). The western shore of Lake Simav has been a swamp throughout most of its Holocene history, but gorge geomorphology encourages strong winds and waves action, which explains the frequent recurrence of facies C-2. Small intermittent flows also develop micro-deltas with typical foreset beds dipping towards the lake (facies C-1) (Blikra and Nemec, 1998).

Peat facies (Facies B) are a significant part of the Boğazköy Trench section (Fig. 6A). Facies B-1 consists of abundant macroscopic fibrous vegetal fragments with some preserved root penetration structures, corresponding to lingo-cellulose material of Boussafir et al. (2012), which we attribute to a paludal environment. In most temperate climates, reed communities can tolerate a maximum depositional depth of 1.5 m (Rodewald-Rudescu, 1974). We suggest this is a reasonable

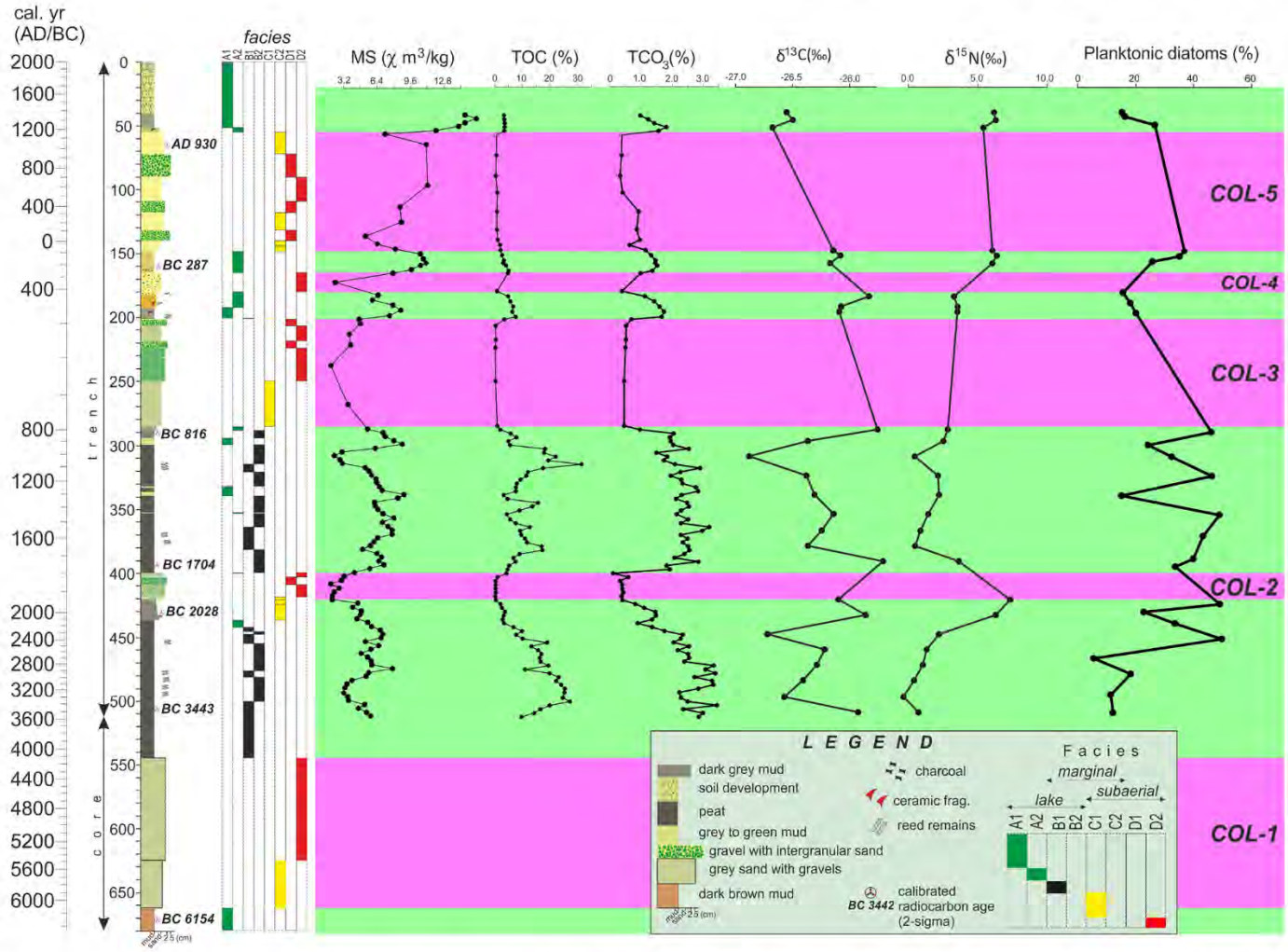

Fig. 7. Vertical change of various proxies in different facies of the Boğazköy Trench. *COL-1* to *COL-5* mark the colluvial packages. See Table 1 for the details of raw and calibrated ages shown and refer to Chapter 5.1.1 for facies explanations.

estimate for paleobathymetry during the deposition of this facies. The finer-grained amorphous organic matter facies (B-2) represents a deeper environment (>1.5–2 m) where abundant allochthonous organic material from the watershed, coastal peat, aquatic microorganism, and finer siliciclastics were transported and deposited (Dean and Fouch, 1983; Boussafir et al., 2012). TOC content of both peat facies is over 10%, and even reaches 30% (Fig. 7). Previous studies in western China have demonstrated that higher TOC content in peat facies is related to humid and warm climates where plant development flourishes (Zheng et al., 2007).

The muddy facies in the trench section differs with regards to the silt to fine sand fraction. Facies A-1 represents muds deposited from suspension settling in deeper water relatively distal from the shoreline. However, exotic gravels are observed in the facies, which can be transported by dense partially submerged mudflows. Frequent vertical stacking of this facies to B-2 and to a lesser extent B-1 may suggest rapid deepening (>2 m) of the lake. However, more silt and fine sand-bearing B-2 facies can also represent the growth of a shoal area as they are often comprised of mollusc and ceramic fragments.

5.1.1.4. Magnetic susceptibility (MS), TOC, TCO_3, ^{13}C and ^{15}N, Planktonic Diatom (PD) ratio

5.1.1.4.1. MS curve. The magnetic susceptibility curve is composed of two main segments. The lower one (250–520 cm) is characterised by a series of small (3.2–6.4 χ) fluctuations (Fig. 7), the largest of which matches with the gravel band at 400–420 cm. Others are confined in peat and mud facies. The upper segment (40–250 cm) shows a progressive increase upwards. Muddy lacustrine facies punctuate this rising trend of MS at 50 cm, 160 cm and 180 cm.

5.1.1.4.2. TOC, TCO_3. Both curves exhibit similar trends (Fig. 7). From the base to the gravel band at 400–420 cm, the *TOC* regularly decreases from 30% to 0% while the decrease in TCO_3 is from 3% to 0%. In the interval 280–400 cm, the *TOC* values display three peaks (ranging from 20 to 30%) with a background value of 10%. In contrast, TCO_3 values show small (<0.5%) variations. The uppermost lacustrine intervals between colluvial wedges at 190 cm, 160 cm, and 40 cm are generally characterised by very small *TOC* (<5%) and TCO_3 (2%) values in concert.

5.1.1.4.3. $\delta^{13}C_{org}$ and $\delta^{15}N$ curves. Both curves display similar trends between 280 and 520 cm. They exhibit increasingly positive values until the gravel bed at 400–420 cm. A slight positive shift occurs above 400 cm in the $\delta^{13}C_{org}$ curve and a typical, yet significant negative shift occurs in both curves around 320 cm. Within the lacustrine facies interlayered between coarse-grained colluvium, the curves diverge from one another where the $\delta^{13}C_{org}$ values become increasingly negative (from −25%0 to −26.7%0) and $\delta^{15}N$ values become increasingly positive (Fig. 7).

5.1.1.4.4. Planktonic diatom (PD) ratio. Between 460 and 520 cm, the PD ratios remain at 15% while upward into the section, between 420 and 460 cm the PD ratio significantly increases (>45%) (Fig. 7). Two

Table 1
Brief description and interpretation of the facies observed in the Boğazköy Trench Section.

Facies type	Facies code	Description	Interpretation
Muddy Facies	A-1	Grey-to-green massive mud (Fig. 3D). Darker colour possible as organic matter increased. Sometimes, silty with cm-sized angular gravels locally. Abundant diatom frustules and rare bivalvia shells included. Frequently alternated with peat facies. TOC <4% and CO_3 < 1% generally.	Deep lake
	A-2	Grey clayey silt/fine sand: more silt/sand grade gives a yellow colour. Comprise locally of abundant charcoal, granule (<0.6 cm) and fragments of mollusc, bone and ceramics (Fig. 3E). Root imprints found locally. Frequently occurs between massive mud and sandy facies.	Shallow lake
Peat Facies	B-1	Fibrous peat: Brown to black in colour (Fig. 3F). Having reed sheath and leafs. Vertical root penetration locally visible. TOC mostly >15%, and CO_3 ~ 2.5%. Frequently associated with massive peat facies.	Shallow wetland
	B-2	Massive fine-grained peat: Composed of very fine amorphous and fibrous fragments almost impossible to distinguish with the naked eye. Easily friable, black in colour. Gradually grades to facies A-1 with grey colour as the clay content rises.	Deeper paludal environment
Sandy Facies	C-1	Cross-bedded sand: grey-to-yellow coloured, well-sorted, medium to coarse sand. Cm-thick foresets with 15–20 cm high, dipping 30^0 towards the lake and alternating with massive sand facies (Fig. 3G).	Gilbert-type micro-delta
	C-2	Massive sand: Well-sorted, grey-coloured, structureless-to-faintly bedded sand (Fig. 3G). Locally partially cemented, including larger (0.5 cm) pebbles. Mostly found between muddy and gravelly facies as thick as 15 to 35 cm. Shows very low MS values and < 1% CO_3 content. TOC up to 4%.	Wave reworking
Gravelly Facies	D-1	Massive gravel: Poorly sorted angular gravels of schist and quartzite. Generally 2–3 cm in size, but larger than 5 cm locally. Intergranular pores filled with silt and finer sand (Fig. 3D). Zero TOC and CO_3 content.	Subaerial debris flow
	D-2	Sandy gravel: Accumulation of finer gravel (<2 cm) and coarse sand with frequent dissemination of angular gravels (>3 cm). Subtle grain-size change vertically resulting in a crude bedding appearance. Higher MS values depending on the clay content.	Waining fluid flow

sharp troughs in the PD ratio match with the B-1 facies, characterised by abundant reed remnants, significant lacustrine intervals between 290 and 400 cm (<25%). We further note that the PD values gradually decrease towards the base of the gravel band at 460 cm, followed by an increase away from the top of the same bed at 400 cm (Fig. 7). The PD ratio also drastically increases in lake facies between 190 cm and 150 cm from 15 to 35%. At the base of the uppermost lake muds, a notable decrease in the PD ratio is also present.

5.1.1.5. Interpretation

5.1.1.5.1. MS curve. Organic matter and carbonates are effectively non-magnetic (Mullins, 1977) whereas the MS of the siliciclastic fraction is determined by the grain size. Furthermore, weathering increases with precipitation (Boggs, 1995), which in turn results in the formation of more clay minerals and higher MS values (Kukla et al., 1988; Maher and Thompson, 1991). The consistent inverse trend between MS and TOC (e.g., 490 cm, 380 cm, 350 cm, 310 cm) confirms that the higher MS values are linked with clay-rich intervals, as a higher lake level increases the amount of suspended sediments in the lake water column. However, an increasingly higher MS signature even in the coarser wedges is also a manifestation of the increasing amount of clay-sized material and hence a wetting of climate up-section (Fig. 7).

5.1.1.5.2. TOC and TCO_3. TOC is comprised of aquatic macro- and microphytes, as well as allochthonous organic matter from the watershed (Meyers and Teranes, 2001). Since the watershed of colluvium in the trench is minimal, the transported organic material can be ignored (Fig. 3A) and TOC can be considered as a good measure of aquatic biomass production and subsequent degradation. The carbonate content of sediments in alkaline lakes is formed from micro- and macro-shells, frustules, and micrite that precipitates biochemically from lake water (Collinson, 1978). Accordingly, higher TOC values mostly correspond to levels of in-situ reed development (B-1 facies) where macrophyte production is highest. In contrast, the lower values correspond to clay-rich allochthonous peat facies (B-2 facies). Moreover, the relationship between *TOC and TCO_3* curves (Fig. 7) likely signifies that the carbonate content is linked with carbonate precipitation on the surface of algae and macrophytes (Ju et al., 2010).

5.1.1.5.3. $\delta^{13}C_{org}$ and $\delta^{15}N$ curves. $\delta^{13}C_{org}$ of lacustrine organic material can be used to trace changes of carbon in terrestrial and aquatic cycles (Leng et al., 2006). Algae and aquatic macrophytes have extremely negative $\delta^{13}C_{org}$ values (−30 to −25‰) as they take up dissolved CO_3 and HCO_3 in lake water, while C4 plants (mainly arboreal cover) mostly display values between −10 to −15‰ (Meyers and Teranes, 2001). $\delta^{15}N$ of lake sediments depend on the type of organic matter (phytoplanktons are N-rich and terrestrial plants are N-poor), but also the pH of lake water (Talbot, 2004). Lower $\delta^{15}N$ values generally indicate higher amounts of cyanobacterial remains and phytoplanktons in lake water (Talbot, 2004). Both curves confirm the prevalence of aquatic macro- and microphytes in TOC. Towards the top and base of the colluvial wedges, COL-2, 3, 4 and 5, both curves exhibit a positive shift that most likely indicates a slight increase in the input of terrestrial organic matter (Fig. 7). This relationship is consistent with a small drainage area. However, above COL-3 the curves diverge. The diverging curves indicate, the lake deepening rapidly at this time resulting in an increase of algae contribution to TOC and a negative shift in $\delta^{13}C_{org}$ curve. Finally, the slight negative shift in $\delta^{15}N$ is likely related to increasing lake alkalinity.

5.1.1.5.4. Planktonic diatom (PD) ratio. Although diatoms are widely used to trace the past hydrologic conditions, using the planktonic/benthonic diatom ratio to understand changes in past lake-levels is relatively new (Wolin and Duthie, 1999; Laird and Cumming, 2008; Wolin and Stone, 2010). A low PD ratio and the presence of abundant in-situ reed remains indicate very shallow conditions between 470 and 500 cm (Fig. 7). All sediment records within the interval 290–450 cm, except COL-2 colluvium itself, generally reflect higher lake levels (PD > 30%). The lacustrine sediments from this time are accordingly composed of mud and allochthonous peat facies that correspond to relatively deeper conditions (Fig. 7). However, two sharp lake level drops are present. The absence of any apparent relationship between $\delta^{13}C_{org}$ and PD ratio (Fig. 7) demonstrates that the latter was primarily controlled by lake level and not ecological processes (such as algal booming) (Wang et al., 2013).

5.1.2. Naşa core

5.1.2.1. Lithology and interpretation. The Naşa core penetrates 18 m into the ground and measures 530 cm thick (average recovery = 30%). Core losses mostly occur in the lower sandy intervals. Considering the time frame of the present study, we studied the uppermost 11 m deep sediments after we corrected for compaction as a result of traditional drilling techniques. The basal interval between 1060 and 840 cm is composed of coarse green sand with infrequent gravels ranging from 3 to 4 mm (Fig. 6C). The overlying interval, from 812 to 844 cm consists of grey-to-green stiff black mud including various diatoms and 2–3 mm carbonate nodules. A 200 cm-long part of the core was lost during drilling between 600 and 812 cm as confirmed by the radiocarbon dating. Up to 576 cm, a diatomaceous and gastropod-bearing black peat interval occurs (Fig. 6C) (see Ocakoğlu et al., 2019a for diatom and mollusc content). The interval from 430 to 576 cm consists of grey to yellow silt/fine sand with abundant planktonic diatom species, indicating a relatively deeper aquatic environment (Ocakoğlu et al., 2019a). Further up-section, a plastic clay interval is observed between 300 and 476 cm, which exhibits a 10 cm thick peat layer and abundant benthonic diatoms at 400 cm. A yellow to cream-coloured plastic mud observed between 210 and 300 cm is overlain by alternating grey and brown mud laminae until 60 cm (Fig. 6C). Finally, the top of the core is sealed by brown and then grey to green mud.

5.1.2.1.1. Interpretation. The basal gravelly sand interval is interpreted as a subaerial environment based on the monotonous coarser grains devoid of diatom/mollusc. Aquatic, possibly wetland conditions settled at 840 cm and lasted up to 580 cm (likely including the missing part). The overlying intervals represent fully developed lacustrine conditions with considerable lake level changes, as indicated by diatom data (Ocakoğlu et al., 2019a).

5.1.2.1.2. Age-depth model. Four radiocarbon ages from charcoal were used to construct the age model in Naşa core (Fig. 6C; Table 2). The earliest lacustrine muds at 836 cm on the basal sands give a calendar age of 11,922 B·C. Following a significant core loss, the peat level at 670 cm yields an age of 6275 BCE Plastic muds above in the middle of the core are undated as they are charcoal-free. However, based on the two radiocarbon dates further up-section (Fig. 6C), we calculated a sedimentation rate in the middle and upper parts of about 0.69 mm y^{-1} – comparable with the rates in the Boğazköy Trench section. Reworking of lake sediments by agricultural activities at the top 10 cm since the late 1950s did not adversely impact the age-depth model because the uppermost radiocarbon date comes from 70 cm of the core (Fig. 6C).

5.1.3. Gölköy core

5.1.3.1. Lithology. The Gölköy core is 9 m deep and has a thickness of 390 cm. It is composed of alternations of coarse and finer lithologies. The compaction-corrected core is shown in Fig. 6B. The very base of the core is composed of gravelly, green sands. Up-section, a rapid fining-upward trend gives rise first to massive grey muds that transitions to dark peat with microscopic macrophytes (facies B-2) at 570–700 cm (Fig. 6B). From 476 cm to 570 cm in the section, a green-to-yellow silt level is present. Until 300 cm the fine-grained peat facies repeats. The overlying interval between 215 and 300 cm is dominated by dark-looking silt/fine sand alternations with infrequent macrophyte fragments. Further up-section, alternating yellow mud and dark grey silt are present. From 70 cm to 124 cm, a green silt/fine sand interval is observed, followed by green-to-grey mud at the top of the core (Fig. 6B).

5.1.4. Interpretation

The basal sand in the core is almost identical to that of the Naşa core

Table 2
Radiocarbon data of the samples from the Boğazköy Trench and Naşa Cores. Initials before labID signify the source laboratories. Geor: Georgia University- USA, SacA: ARTEMIS- France, Beta: Beta Analytical-UK.

	Sample ID	Lab ID	Material	δ13C (‰)	^{14}C age, years BP	Cal. Age (1 s)* (A.D./B.C.)	Mean cal age
NAŞA CORES	N-68	Geor 29,431	Sediment	−28.16	2030 ± 25	12 CE- 48 BCE (%100)	30 BCE
	N-188	Geor 29,432	Peat	−28.61	2650 ± 25	797–819 BCE (%100)	810 BCE
	NAS2/189–191	SacA44428	Peat		2365 ± 30	434–472 BCE (%39) 393–423 BCE (%61)	400 BCE
	N-290	Geor 29,433	Charcoal	−24.85	7370 ± 30	6314–6339 BCE (%18) 6217–6257 BCE (%47) 6093–6139 BCE (%34)	6245 BCE
	N-350	Geor 29,434	Peat	−26.15	12,020 ± 30	11,855–11,926 BCE (%55) 11,974–12,020 BCE (%31) 12,031–12,054 BCE (%14)	11,922 BCE
	BOG 67	SacA 44,167	Charcoal	−30.4	1150 ± 30	917–974 CE (%61) 878–900 CE (%25)	930 CE
	BOG 160–164	SacA 44,168	Charcoal	−24.6	2195 ± 30	331–280 BCE (%47) 232–197 BCE (%31) 356–334 BCE (%19)	287 BCE
	BOG 184–188	SacA 47,715	Peat	−30.4	2230 ± 60	316–204 BCE (%79) 381–346 BCE (%22)	276 BCE
	BOG 200–202	SacA 47,716	Charcoal	−30.4	2255 ± 30	282–231 BCE (%58) 387–354 BCE (%42)	280 BCE
	BOG 288–291	Geor 25,517	Charcoal	−24.6	2650 ± 30	831–801 BCE (%100)	816 BCE
BOĞAZKÖY TRENCH	BOG 288–291	Beta451315	Charcoal	−25.1	2660 ± 30	831–797 BCE (%100)	818 BCE
	BOG 356	Beta 451,316	Charcoal	−26.0	3230 ± 30	1769–1687 BCE (%85) 1866–1851 BCE (%11)	1728 BCE
	BOG 391–394	SacA 47,717	Peat	−30.4	3410 ± 50	1750–1623 BCE (%94)	1704 BCE
	BOG 430–433	SacA 44,427	Peat	−25.3	3655 ± 30	2128–2092 BCE (%34) 2041–2009 BCE (%34) 2002–1972 BCE (31)	2028 BCE
	BOG 506–508	Geor 25,518	Charcoal	−26.6	4680 ± 25	3462–3423 BCE (%45) 3514–3492 BCE (%26) 3411–3394 BCE (%18)	3443 BCE
	BOG 509–512	SacA44169	Organic mud	−26.1	3585 ± 30	1962–1892 BCE (%88) 1972–1966 BCE (%5)	1939 BCE
	BOG 669–672	Beta451317	Organic mud	−26.6	7420 ± 30	6216–6142 BCE (%78) 6092–6073 BCE (%22)	6154 BCE
	BOG 672–675	SacA 47,718	Organic mud	−30.4	7150 ± 35	6033–5991 BCE (%74) 6057–6042 BCE (%25)	6022 BCE

* Stuiver et al., 2021, Intcal20, Calib Rev. 8.2.0.

– indicating a subaerial depositional environment. The segment of the core up to 300 cm represents a relatively deep (>2 m) environment based on the modern analogs of allochthonous peat discussed earlier. The silty interval between 480 and 570 cm likely represents shallower conditions, closer to the paleo-lakeside. The remaining upper part of the core generally corresponds to a deeper lake environment. However, siliciclastic wedges at 220–300 cm and 70–120 cm coincide with times when the lake level presumably dropped.

6. Lake level changes

The Holocene basin-fill is shown in a horizontally non-scaled *E*-W geological section in Fig. 8. This figure relies on the cm-resolution elevation measurements on top of the sections and the lithology and thickness of the facies observed. The timelines were drawn according to the age model in the Boğazköy Trench (Fig. 5A). These ages were then linearly interpolated and correlated with the radiocarbon ages in the Naşa Core. As demonstrated in Section 5.1.1, the boundary between the coarse-grained wedges and the lacustrine facies signifies the past lake level elevation at that stratigraphic level in the Boğazköy Trench section. One can therefore predict the lake depth at these times by combining this data with the depth of the same stratigraphic level, derived from the age model of the Naşa core in the lake centre. When we encountered a subaerial coarse-grained wedge, we know the lake level must have been below this stratigraphic level. However, we cannot quantify how much shallower the lake was due to the paucity of our drilling locations. In this light, lake levels and the corresponding magnitudes of calculated precipitation at the base and top of colluvial wedges should be considered maximums. Moreover, the landward extent of the lake facies is unknown due to the overlying colluvial cover. Nevertheless, a distinct but still unmappable flat surface at the lake margin near Boğazköy Trench at 785 m is traceable at the top of the gorge (Fig. 4A). Moreover, a notable sandy/silty zone is present along the paleo-shoreline (Fig. 3A). The clayey silt facies, exotic gravels and ceramic fragments in the mud facies and especially leafy peat facies strongly imply very shallow (1–1.5 m) water depth whereas the fine-grained peat and muddy facies indicate the transition to deeper (>2 m) water. At this time, it is likely that Lake Simav drained through the Boğazköy and Ortaboğaz gorges (Fig. 4B). The facies interpretation coupled with the fluctuations in the proxies (Fig. 7) tracks general changes in the lake level with time. Accordingly, we suggest very shoal lake conditions (max. 220 cm) between 640 and 545 cm (COL-1) followed by an increase in lake level until 420 cm. In this lacustrine sequence, the intervals 500–550 cm and 440–470 cm seem to represent relatively deeper lake conditions, consistent with the observed facies and increase in MS and PD ratio (Fig. 7). In contrast, the interval from 470 to 510 cm corresponds to lower lake levels (<1.5 m at lake margin) based on abundant in-situ reed fragments, higher TOC and lower PD values (Fig. 7). After the lake margin exposure in COL-2 (400–420 cm), the lake level fluctuated several times until 285 cm. The most notable shoaling event in this interval occurs around 320 cm, which is characterised by the highest TOC and lowest MS values (Fig. 7). Finally, the three colluvial levels (COL-3, 4 and 5) demonstrate renewed subaerial exposure at the trench location along the westernmost lake margin, which were in turn inundated at about 50 cm, based on overlying lacustrine facies (Fig. 7). Table 3 summarises the lake level and depth data belonging to the base and top of the colluvial wedges and the lacustrine facies with known paleobathymetry.

7. Application of hydro-balance model to simav area

7.1. Simav runoff data

According to the DSI meteorological data (Tables S1-S3), the monitoring period consists of a ten-year long (1979–1988) humid ($P > 600$

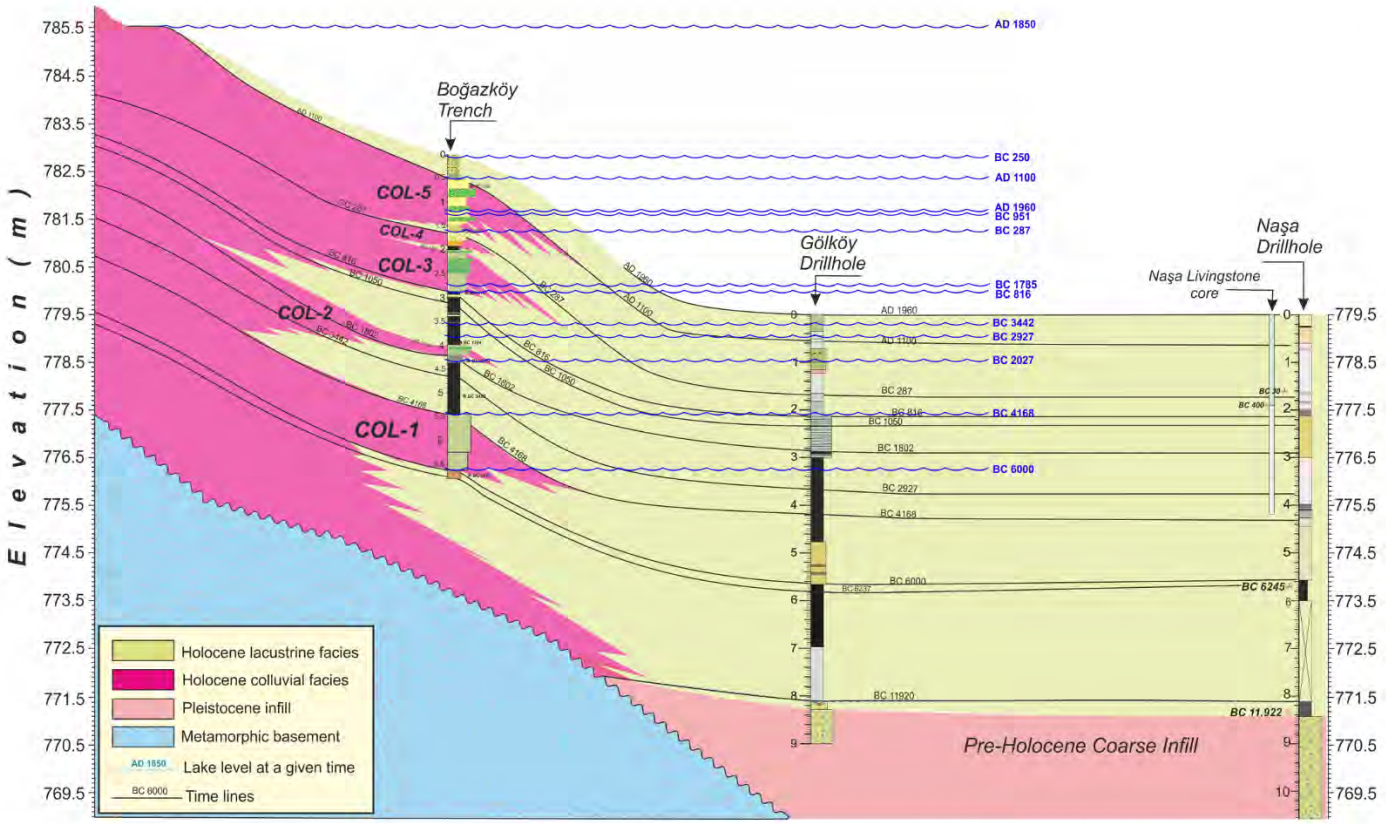

Fig. 8. Longitudinal *E*-W geological section connecting the colluvial facies to the lacustrine facies. Blue wavy lines depict past lake levels whereas the black lines show the past lake floors. (For interpretation of the references to colour in this figure legend, the reader is referred to the web version of this article.)

Table 3
Paleohydrologic data and estimated annual precipitation for different timelines in Lake Simav used for Figs. 8 and 10. Data in bold lines are derived from either the base or top of the colluvial wedges. MTWA: Mean Temperature of Warmest Month.

Time (AD/BC)	Δ T (MTWA)	Lake level altitude (m)	Lake base altitude (m)	Max. lake depth (cm)	Lake volume (10^6m^3)	Lake surface (km^2)	Estimated rainfall (mm)	Run-off coef.	Surface flow (10^6m^3)	Lake surface evap. (10^6m^3)
1960 CE	0	781,00	779,50	150	22,29	17,33	814	0,196	72,7	15,0
1850 CE	0	785,50	779,40	610	130,18	31,68	>553	0,110	27,5	27,4
1100 CE	−0,5	782,40	778,85	355	61,95	22,03	<491	0,083	18,5	18,4
250 BCE	0,4	782,80	777,75	505	99,59	26,53	>528	0,099	23,8	23,6
287 BCE	0,4	781,20	777,78	342	60,25	21,77	<498	0,086	19,5	19,4
816 BCE	−0,5	779,95	777,37	258	42,73	19,99	<478	0,077	16,7	16,7
951 BCE	−0,5	781,60	777,25	435	81,83	24,48	>506	0,089	20,6	20,5
1050 BCE	−0,5	780,75	777,15	365	64,36	22,39	<493	0,084	18,8	18,7
1768 BCE	−0,9	780,10	776,70	340	59,84	21,71	<485	0,080	17,6	17,6
1802 BCE	−0,9	778,60	776,60	200	31,55	18,85	<468	0,072	15,3	15,3
1802 BCE[a]	−0,9	778,10	776,60	150	22,43	17,43	459	0,068	14,1	14,1
2027 BCE	−0,5	778,52	776,40	212	33,74	19,07	>472	0,074	15,9	15,9
2927 BCE	−0,9	779,05	775,70	335	58,69	21,58	>484	0,079	17,5	17,5
3442 BCE	−0,9	779,30	775,32	398	72,95	23,51	>496	0,085	19,2	19,1
4168 BCE	−1,4	777,40	775,20	220	35,38	19,32	<466	0,071	15,1	15,1
6024 BCE	−2	776,25	774,05	220	35,24	19,24	<460	0,068	14,3	14,3
11,920 BCE	−2	773,60	773,60	0	13,00	14,50	<433	0,054	10,7	10,8

[a] Assumes that the precise lake level is 50 cm below the colluvium-lake sediment contact.

mm) period followed by a drier (P < 550 mm) period (1989–1992) (Fig. 9A). In particular, the more humid period is characterised by abundant winter (and partially spring) precipitation, with RC values ranging from 0.25–0.30 (Table S5). Nevertheless, the drier period received more spring (and secondarily winter) precipitation along with significant summer/autumn rainfall. As a result, the RC values occupy a

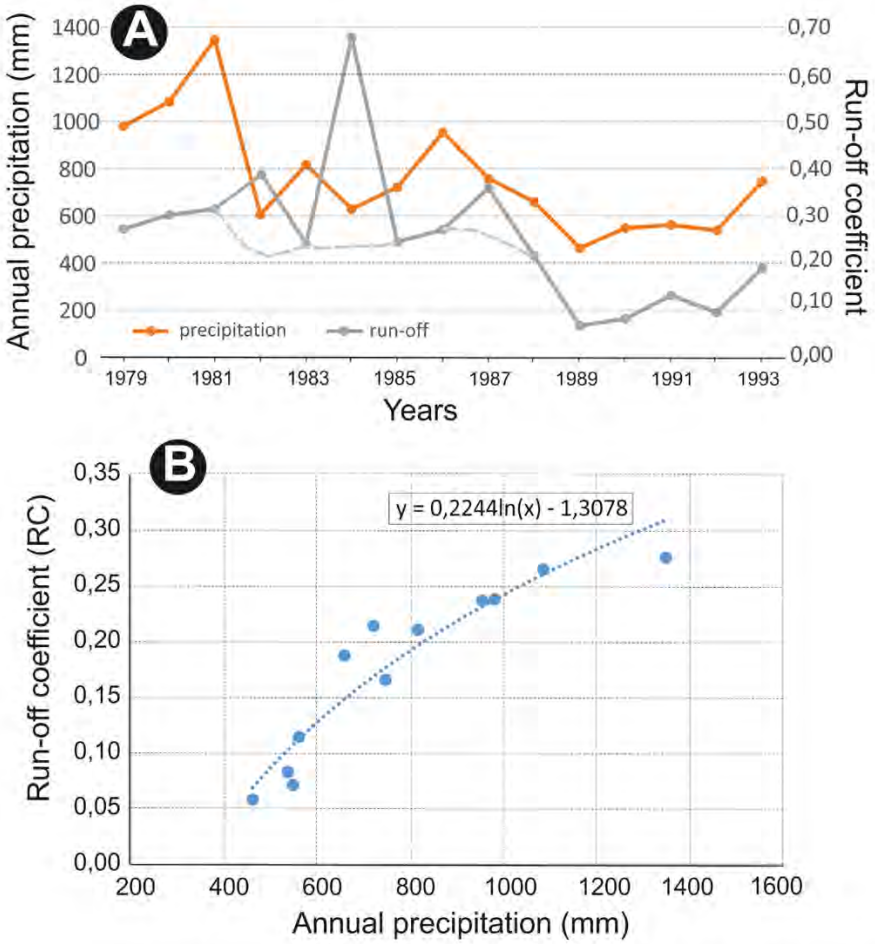

Fig. 9. (A) Yearly runoff rate vs annual precipitation between 1978 and 1993 in the Simav Graben watershed. The dashed line shows the overall trend of runoff (B) The correlation between run-off coefficient and annual precipitation in the same period excluding three anomalous years.

narrow band between 0.06 and 0.11. Fig. 9B and Table S4 demonstrate a strong correlation ($R^2 = 0.89$) between P_{ann} and RC when three anomalous years are discarded (Fig. 9A). Accordingly, the driest year of the record (462 mm in 1989) has RC value of 0.058 while the more humid (561 mm) year of 1991 displays a slightly higher RC value (0.114). The highest RC values (0.25–0.30) are typical of very humid years with P_{ann} over 1000 mm. Later on, we use Fig. 9B to predict the RC and precipitation amount matching the calculated flow in certain past timelines (Table S7).

7.2. Past lake volumes and precipitation estimations

We calculated the surface area and volume of Lake Simav for 16 distinct periods from the latest Pleistocene to 1960 CE based on the basin-fill profile data given in Fig. 8 (Table 3). Most of these timelines closely correspond to the past shorelines based on the contact between the colluvial wedges and lacustrine deposits in the trench section. Since the lake depths are always below the critical threshold of 4.5–5 m (Fig. 4B; Table 3), we confirm the endorheic nature of Lake Simav throughout these timelines. The remaining timelines correspond to the contact between peat and mud facies whose paleobathymetric significance was discussed earlier.

Table 3 shows that the surface flow (72.7 million m^3) significantly exceeded the estimated evaporation from the lake surface in 1957 CE just before the desiccation of Lake Simav. This data is also confirmed by the local people who eyewitnessed the outflowing of the lake via the Boğazköy Gorge. The highest Holocene lake level (depth = 6.10 m) was in 1850 CE, despite the evaporation from the lake surface also being the highest (Table 3). At this time, most of the inflow left the lake via the Boğazköy Gorge in the west and Ortaboğaz Gorge in the north. Outflow from the Ortaboğaz Gorge is further confirmed both by local narratives and the laminated sediments encountered in the upper part of a shallow core in the gorge (Ocakoğlu et al., 2019a). Furthermore, spring precipitation and snow melts were presumably excessively high to threaten the inundation of lake-margin villages such as Boğazköy, Çitgöl and Gölköy (Fig. 2). Ultimately, it is likely that this threat drove Ahmet Vefik Pascha to order the deepening of the Boğazköy Gorge in 1866 (see earlier discussion).

The earliest record of Lake Simav begins in the latest Pleistocene (around 11,920 BCE) and shows a wetland in the centre of the depression (Fig. 8). This environment implies insufficient surface runoff compared to evaporation, despite our model yielding 433 mm of annual precipitation at this time (Table 3). After a quite humid period during the early Holocene when the lake was most probably exhorheic, the modeled maximum annual precipitation at the bottom (6000 BCE) and top (4168 B·C) of COL-1 is 460 mm and 466 mm respectively. It is obvious that the precipitation remained always below these values between 6000 and 4168 BCE Similarly, the precipitation was always below 468–485 mm during the deposition of the COL-2 between 1768 and 1802 BCE (Table 3). If the lake level was precisely 50 cm below the colluvial boundary around 1800 BCE (max. Water depth of 150 cm), a realistic assumption for precipitation is as low as 459 mm, based on the overall morphology of the colluvial wedge in Fig. 7 (Table S7). The minimum annual precipitation between these two drought events is estimated to be 484–496 mm. The subsequent droughts in 816 BCE (base of COL-3) and 1050 BCE (i.e., the notable shoaling observed at 310–320 cm) experienced maximum precipitation of 478 mm and 493 mm respectively (Table 3). At 1100 CE, the maximum precipitation at the top of COL-5 is estimated to be 491 mm. Later on, the precipitation rapidly increased and reached the higher modern values of >800 mm.

8. Discussion

8.1. Colluvial wedges and dry periods

A climate shift towards drier conditions is expected to cause the weakening of the vegetation cover and especially increases the frequency and efficiency of catastrophic rainfall events. In turn, catastrophic rainfall events increase surface runoff and result in enhanced colluvial accumulation of prograding wedges into the lake. We observe the repetition of this conceptual frame many times along the Boğazköy lake margin. Sedimentation rates are also higher during these colluvial depositions (Fig. 5B). Although there is strong evidence for reduced soil formation and hillslope erosion traversing from semi-arid regions to deserts (Owen et al., 2011), the modern monitoring studies across the globe cannot demonstrate a meaningful change in sediment dynamics between semi-arid and humid belts (Riebe et al., 2004; Richardson et al., 2019), most probably due to the complexity of environmental parameters involved. However, model studies suggest that hillslopes become more susceptible to erosion below 500 mm of precipitation in the course of aridification and expose to 2–4 times more erosion at 250–400 mm precipitation depending on the texture of the soil (Istanbulluoglu and Bras, 2006). The field studies demonstrate hillslope erosion rapidly increases while passing from the humid system to the arid ecogeomorphic system of the Mediterranean (Lavee et al., 1998). Similarly, NW Mediterranean long-term Holocene records confirm the increased sediment dynamics in dry periods irrespective of human intervention (Bellin et al., 2013). Therefore, we suggest that the five colluvial packages sandwiched between lake sediments represent five events (dry periods and/or increased local human activities) in the Holocene (Fig. 10A). Here, we expect a time gap between the onset of the colluvial deposition based on the location of the Boğazköy trench section with respect to the lake shoreline. Changes in the proxy records of the lake sediments can further shed light on the precise onset of these events. For instance, the dry period that resulted in the formation of the colluvial package deposited around 816 BCE would have started earlier at 900 BCE (at 300 cm) based on the notable trends in TOC, MS and PD ratios (Fig. 7). Furthermore, there is another dry event at about 1100 BCE (320 cm) displayed in some proxies. However, the strength of this drought was probably not enough to develop a colluvial wedge in the trench section. Similarly, the dry period which is responsible for the colluvial wedge (COL-2) between 400 and 420 cm, likely initiated at 460 cm (i.e. 2150 BCE).

The drought interpretation above based on the presence of colluvial wedges and the Lake Simav record, in general, is consistent with existing Anatolian and neighboring climatic records. It seems that prior to the first colluvium (COL-1), a humid phase began just after 14 ka in the area, which is further supported by the facies in the Gölköy Core (Figs. 6B, 8). Previous studies in the eastern Mediterranean (Eastwood et al., 2007; Jalut et al., 2009; Dormoy et al., 2009; Marino et al., 2009; Dean et al., 2015) and from Lake Van (Landmann et al., 1996) in eastern Anatolia indicate that more humid conditions started 14.6 ka to 10 ka, and prevailed until 8.0 ka to 7.5 ka depending on the geographic position. In the Lake Eski Acıgöl isotope record, the dry period started precisely at 8.3 ka and lasted for 300–400 years (8.2 ka event). Following a relatively long (500 yr) humid period, drier conditions prevailed again until 4000 BCE (Dean et al., 2015). The first prominent shoaling event in Lake Simav occurred around 8.2 ka as amorphous peat was replaced by insitu reed peat in the lake interior and colluvial wedges prograded (COL-1) over lake muds along the lake margin (Fig. 8). This dry period continued until 4000 BCE and was defined by limited lake level fluctuations at the lake's centre (Ocakoğlu et al., 2019a). The composite isotope curve of $\delta^{18}O$ compiled from Eski Acıgöl (Roberts et al., 2001) and Lake Nar (Dean et al., 2015; Jones et al., 2006) reasonably represents the water balance in Central Anatolia and shows an overall positive shift between 5500 and 4000 BCE when lowermost colluvial wedge was active (Fig. 10B). Similarly, the Lake Gölhisar $\delta^{18}O$ isotope record displays a sharp positive shift from 6000 BCE to 5700 BCE, and large deviations (unstable climate conditions) until 4300 BCE (Fig. 10C).

The colluvial wedge dated at around 2000 BCE seems to match reasonably well with the 4.2 ka event and is defined by the most positive $\delta^{18}O$ values of the entire Holocene in Eski Acıgöl and Lake Nar composite record, broadly consistent with the Lake Gölhisar record, albeit

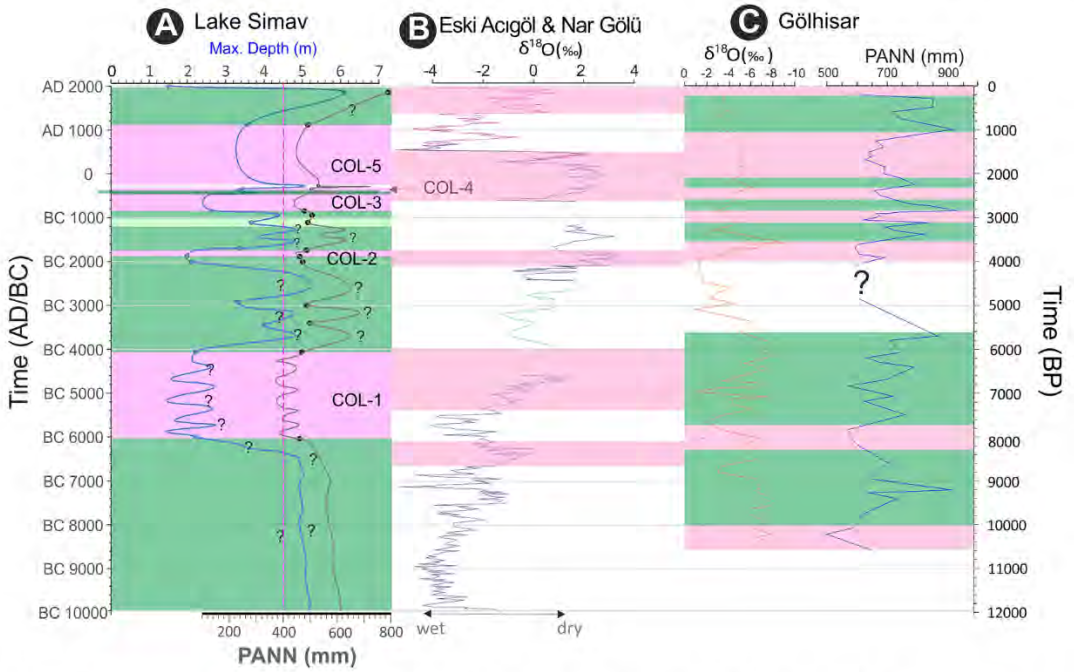

Fig. 10. A- Change in water depth and estimated annual precipitation in Lake Simav. Black dots indicate the estimation timelines. The vertical red dashed line marks the lake depth below which the lake is endorheic. B- Composite $\delta^{18}O$ curve from the central Anatolia (Lake Nar: Blue line (Dean et al., 2015), Red line (Jones et al., 2006), Lake Eski Acıgöl: Green line (Roberts et al., 2001). C- Lake Gölhisar $\delta^{18}O$ and pollen-derived annual precipitation curves (Eastwood et al., 2007). Purple and green bands depict relatively dry and wet periods. (For interpretation of the references to colour in this figure legend, the reader is referred to the web version of this article.)

with slight time shifts (Fig. 10B, C). The shoaling at 1050 BCE and 800 BCE in COL-3 match precisely with the dolomite rich (>20%) interval (3100–2604 yr B.P. and 2500–2300 yr B.P.) that is interpreted as a long dry period in Lake Nar record (Dean et al., 2015). Similarly, the lower part of COL-4 between 200 BCE - 1000 CE displays a good fit with the isotope record, however, after 400 CE the records are no longer consistent. Moreover, although a positive shift in the Central Anatolian record is present around 1000 CE, a continuous record of lake sedimentation is observed in the trench section (Fig. 10B). This diachroneity can be explained by either different microclimate patterns or anthropogenic impacts between central and western Anatolia.

Apart from these very high-resolution paleoclimate records, the period of 3500–2500 BCE in the Kureyşler Valley, 100 km to the east exhibits a positive shift of $\delta^{18}O$ (pedogenic carbonate) and an increase in TOC (Ocakoğlu et al., 2019a), which are compatible with higher lake levels in Lake Simav. Moreover, colluvial wedges at 3.8 ka and 2.9 ka match well with $\delta^{18}O$ shift and MS peak in the terrestrial Kureyşler record. Similarly, the Lake Mogan pollen record (Ankara, Central Anatolia), a counterpart to COL-3, exhibits relatively dry steppe conditions between 3000 and 1500 yr B.P. following a short but complete desiccation (Oybak-Dönmez et al., 2021). The same record reveals a sharp increase in humidity at about 1100 CE, closely correlated to contemporaneous lake level increase in Lake Simav. From 600 B.C.to 1200 CE (except 200–700 CE) in Lake İznik to the north, is broadly considered to be dry (Ülgen et al., 2012) which fits reasonably well with the uppermost Boğazköy colluvial wedge. However, the cold and dry period that starts by 1300 CE in Lake İznik surprisingly corresponds to higher levels in Lake Simav. Lake Tecer, located in eastern Anatolia (Kuzucuoğlu et al., 2011) shows a very poor correlation to the Simav record. The only common event (4.2 ka) is represented by a hiatus between 4300 and 3850 yr B.P. as a result of drought in Lake Tecer. Similarly, dry events (1.8–2.1 ka, 3.3–3.7 ka) and wet events (2.1–3.3 ka, 3.7–4.9 ka) in the eastern Anatolian Lake Hazar (Eriş et al., 2018) have no apparent counterparts to the Lake Simav record. We attribute the lack of continuity between the sites to be a result of different paleoclimatic thresholds recorded by different proxy records.

Although detailed local archaeological records are lacking, close parallels between the climatic proxies in the temporally well-constrained central and SW Anatolian records, indicate climate was the dominant control on the development of the Simav colluvial wedges. However, we concede that we can not completely ignore the impact of human activities on sediment dynamics, which are particularly became pronounced in the dry periods (Dusar et al., 2011). On the other hand, the sedimentation rates in the Black Sea where the Lake Simav catchment debouches began to increase around 200 BCE (Walling (2006) based on Degens et al. (1991)). The author interpreted this increase as the result of land clearance and intensified agricultural activities. Thus, the colluvial wedge COL-5 is likely a result of human impact in Hellenistic to Byzantine periods. Furthermore, this coincides with the earliest appearance of ceramic fragments in the Boğazköy trench (Fig. 6A).

8.2. *Absolute precipitation estimates*

The majority of paleoclimatic proxies enable the correlation of relative change in temperature and precipitation with time. Nevertheless, the knowledge of the absolute values of these parameters seems to be very significant for both the magnitude of past climate changes and the quantification of their impact upon ecology and human culture. Because temperature changes were minimal (<2 °C) throughout Holocene, the target of quantification is generally precipitation. In the literature, pollen transfer functions were applied for both P and T (Davis et al., 2003; Eastwood et al., 2007; Dormoy et al., 2009; Jalut et al., 2009; Pross et al., 2009), chironomids were used as a proxy for T (Dieffenbacher-Krall et al., 2007; Tóth et al., 2015), hydrological balance models were used as a proxy for P (DeVogel et al., 2004; Bookhagen et al., 2001; Junginger and Trauth, 2013), which were together integrated within hydrology/isotope (Polissar et al., 2006; Lacey and Jones, 2018) and back-analysis global climate (Kutzbach and Guetter, 1986; Kutzbach et al., 1993; Arıkan and Yıldırım, 2018) models.

Quantitative paleoclimate estimates in Anatolia and the vicinity is

scarce. Using hydrological and isotopic investigation in an Albanian lake, Lacey and Jones (2018) presumed annual precipitation of 432 mm at 14 ka. They also suggested that the precipitation was 26% greater in the early Holocene than the modern magnitudes (773 mm). Dormoy et al. (2009)'s pollen-based annual precipitation estimation in the northern Aegean for the Older Dryas at 14 ka is 430 mm. For the early Holocene optimum they suggested higher (about 750–800 mm) values. In their model, the precipitation sharply dropped to 600 mm at 8.2 ka during the end of the Holocene optimum. Similarly, Pross et al. (2009) suggested increased seasonality and 25% less precipitation (a drop from 800 mm to 600 mm) during the 8.2 ka event. Eastwood et al. (2007) produced an almost continuous pollen-based precipitation record from Lake Gölhisar (SW Anatolia) depicting a sharp fluctuation between 550 mm and 900 mm, which encapsulates the actual value of about 600 mm.

The two remaining quantitative estimates in the literature are from the southern Levant. Calibration of the $\delta^{18}O$ stalagmite record with recent precipitation data demonstrates that precipitation dropped almost 400 mm (50%) in 5700–5600 yr B.P. compared to earlier (Bar-Matthews and Ayalon, 2011). Frumkin (2009), similarly suggested that precipitation decreased 50% in the Dead Sea region around 4.2 ka, based on $\delta^{13}C$ series calibrated with current climate data from a *Tomarix* fossil trunk.

Quantitative precipitation estimates derived from the past water balance of Lake Simav display striking similarities to the studies above. Before the settlement of lacustrine conditions at 12000 BCE, we calculated a precipitation magnitude of <433 mm, which is comparable to the Albanian and North Aegean records. The lowermost colluvial wedge (COL-1) abruptly overlies the lacustrine muds, likely indicating a rapid lake level drop (Fig. 8). The estimated precipitation around 8 ka is below 460 mm (Table 3; Fig. 10A). Our model also suggests that throughout the deposition of this colluvium between 6 and 8 ka, the annual precipitation never exceeded 460–466 mm. This value is considerably smaller compared to 600 mm obtained from the North Aegean pollen records (Pross et al., 2009; Dormoy et al., 2009). The Lake Gölhisar record shows a gradual decline in precipitation after 8.5 ka to 600 mm around 7.9–8.0 ka (Eastwood et al., 2007) (Fig. 10C).

After a relatively humid 2000 yr, we suggest a precipitation magnitude of <468 mm at the onset of 4.2 ka event around 1800 BCE For the same period, Arıkan and Yıldırım (2018) suggested 420–430 mm of annual precipitation in Delice Valley (Central Anatolia) using the downscaling of Macrophysical Climate Model (Bryson and DeWall, 2007). Strikingly, in Lake Gölhisar, between 3.6 and 3.8 ka, the annual precipitation was one of the lowest in the Holocene and perfectly fits the development of the COL-2 wedge in Lake Simav (Fig. 10A). According to the proxy data in the trench section, this event started at 440 cm into the section at exactly 4.2 ka. Earlier, the area received more precipitation (>500 mm) as evidenced by higher lake levels at around 3400 BCE (Fig. 10A). However, it seems as if the fluctuating precipitation was subdued to as low as 490 mm during this high-stage lake level between 6 and 4.2 ka (Table 3).

Later, the precipitation first dropped below 493 mm (at about 1050 BCE) causing a notable shoaling, and then further decreased below 478 mm at around 816 BCE giving rise to the colluvial wedge COL-3 in the Simav area. Arıkan and Yıldırım (2018) suggest precipitation for the semi-arid north-central Anatolia region was only 400 mm at this time. The period between 800 and 1200 BCE in Lake Gölhisar is also a pronounced dry period, as precipitation dropped as low as 650 mm (Eastwood et al., 2007) (Fig. 10C). At 250 BCE, just before the onset of the uppermost colluvial package, precipitation is the highest (>528 mm) in the Holocene and strictly coincides with the Roman Warm Period. Furthermore, the appearance of lacustrine muds over colluvium (COL-4) in the Boğazköy trench section is compatible with the Medieval Warm Period (Mann, 2002), which is characterised by very high temperatures, similar to the 20th century. This particular period starts at 287 BCE in the Bereket Plain (Kaniewski et al., 2007) and is known to be a cultivation period in the nearby Gravgaz lowland (Vermoere et al., 2000). Similarly, the period between 100 and 300 BCE is relatively humid (775 mm) in the nearby Lake Gölhisar record (Eastwood et al., 2007) (Fig. 10C). The subsequent Byzantine Period matches exactly with the uppermost colluvial wedge (COL-5) and spans 400/450–1000 CE This was a time of widespread land abandonment in Cappodocia (central Anatolia) (England et al., 2008). There is a positive shift of $\delta^{18}O$ after 700 CE, which was interpreted as a sign of drought in Cappodocia (Jones et al., 2006). The southerly record of Lake Gölhisar indicates that the latest Roman-Byzantine period was also drier (650 mm) compared to the periods before and after (Eastwood et al., 2007). Here, the subsequent humid period -one of the wettest of all Holocene- starts at 1000 CE which is temporally very close to the Lake Simav wetting period at 1100 CE At this time, the precipitation gradient between Lake Simav (491 mm) and Lake Gölhisar (900 m) persisted and remained through the entirety of the Holocene.

8.3. Archaeological implications

The Holocene is marked by several climate events that are characterised by widespread and severe droughts (Bond et al., 1997; Mayewski et al., 2004). In West Asia, where prehistoric and historic groups alike mostly relied on rain-fed cereal agriculture for their subsistence, such drops in precipitation significantly affected the political and social configurations (Staubwasser and Weiss, 2006). In Anatolia, the resolution of climate data in conjunction with the archaeological record remained limited for a long time. However, recent multidisciplinary investigations in western Anatolia have changed this situation substantially, providing high-resolution geoarchaeological and climatic data concerning past societies (Groenhuijzen et al., 2014; Roberts et al., 2018; Ocakoğlu et al., 2019b).

The Lake Simav data add to the current picture of past human-climate interactions in western Anatolia. Unfortunately, the direct correlation of paleoclimatic data with archaeology is extremely difficult as local archaeological proxies are lacking. Therefore, our interpretations will rely on studies from neighboring areas of western Anatolia and should be treated as tentative.

The estimated annual precipitation from ca. 6500 BCE onwards (Fig. 10A) allows data-driven insights into the long-term changes in the social and political organization under oscillating climatic conditions. It is known that variability in interannual rainfall in west Asia was a significant factor that impacted human societies. To this end, inner western Anatolia may have been one of the areas where such fluctuations occurred, indicating droughts likely influenced agricultural output in a negative manner (Massa and Şahoğlu, 2015).

Annual precipitation rates from Lake Simav indicate that the precipitation has never dropped below 250 mm/year indicating the dry farming threshold has never been exceeded. However, there are multiple episodes where rainfall rapidly diminishes in the paleoclimatic record (Fig. 10A). In detail, major events where climate change rapidly occur at 8.2 ka, 4.2 ka, and 3.2 ka – although some variability in timing is observed regionally. The Early Holocene is a period of wetter and warmer climate than the Mid and Late Holocene (Kuzucuoğlu, 2002; Dormoy et al., 2009; Pross et al., 2009). In the Simav area, the 8.2 ka event is stratigraphically manifested at 8000 cal. yr B.P., with a relatively low estimated annual rainfall of <460 mm (Fig. 10A). Dry conditions (always $P < 466$ mm) persisted with some wet spells until 4100 BCE This sort of aridity would have been problematic for prehistoric farmer-herder groups in the region, who presumably relied almost entirely on rain-fed agro-pastoral economies for their subsistence (Bogaard, 2005; Marston et al., 2021). The faunal record indicates that after cal. 6000 BCE, west Anatolian farmer-herders began to incorporate alternative food sources into their diet by increasing the consumption of marine resources, dairy products, and game meat (Çakırlar, 2012a, 2012b; Horejs and Galik, 2011). Whether there is a meaningful correlation between the increased aridity around 8.2 ka and the slight shift in subsistence strategies remain to be explored further.

The area, where Lake Simav is located, has been poorly researched with regards to the Neolithic period. Akmakça and Fındık Kayabaşı are two major sites that are dated to the late seventh millennium B.C. by pottery comparisons to Hacılar IX-VI (Efe, 1995). Similar sites can be found in the neighboring provinces of Uşak, Eskişehir, and Bilecik where recent fieldwork identified multiple 7th and 6th millennia B.C. localities (Efe et al., 2012; Fidan et al., 2020; Yılmaz, 2020; Yılmaz, 2020). Unfortunately, the lack of high-resolution radiocarbon dating from these sites and the fact that most are only known through surveys impede a direct correlation of Lake Simav rainfall data to the early farmer-herder response to the changing climatic conditions. As mentioned above, current evidence suggests that the communities did not abandon settlements following this aridity phase, but instead seem to adapted to new conditions by increasing the amount of wild fauna and marine resources into their diet.

One of the implications of the precipitation curve from Lake Simav is the gradual and continuous increase in precipitation from ca. 4000 BCE onwards, which peaks several times until 3000 BCE (Fig. 10A). Very similar observations were also made on multi-proxy data collected from the Kureyşler area (Ocakoğlu et al., 2019b). This gradual increase in rainfall coincides with the Late Chalcolithic and Early Bronze *Age* I period in western Anatolia, which is characterised by the establishment of new settlements, the appearance of centralised and fortified places, and a re-organization of the political structure (Çilingiroğlu and Ünlüsoy, 2017; Schwall and Horejs, 2020) including: Troy, Küllüoba, Beycesultan, Bakla Tepe, and Liman Tepe (Şahoğlu, 2005; Efe, 2007; Ünlüsoy, 2018). Based on the data extrapolated from Lake Simav, one can establish a positive correlation between the increased precipitation and the upsurge in settlements. Optimizing agricultural production may have played a role in the establishment of new settlements, major building projects, a stable political atmosphere, and a possible increase in population size, which culminated with increasing social complexity in western Anatolia.

The 4.2 ka event is one of the most rapid climate change events whose effects can be observed in the archaeological record globally. The 4.2 ka event lasts ca. 300 years from cal. 2200–1900 BCE (Weiss, 2017; Kaniewski et al., 2018). This extremely arid phase impacted Bronze Age communities across west Asia including Anatolia (Massa and Şahoğlu, 2015; Ocakoğlu et al., 2019b). Already in the mid-third millennium B.C., we observe a decrease in rainfall in the Lake Simav data, which predicts a significant decrease in precipitation, with <468 mm (even 470 mm, see Chapter 7.2) annual rainfall at 1800 BCE (Fig. 10A). In this respect, it is interesting that settlement mounds around Kütahya such as Ortaca and Höyüktepe were abandoned prior to the mid-third millennium B.C. (Türktüzün et al., 2014, 2015a, 2015b). It is unclear whether there is a meaningful relationship between the low rainfall and the abandonment of multiple sites in the Kütahya region around this stage. However, the paleoclimatic data indicates that this possibility is worth further research.

The Early Bronze Age III central site of Seyitömer (Kütahya) was destroyed by a severe fire event around cal. 2220 BCE and it is an interesting case for assessing the impact of the 4.2 ka event in western Anatolia (Harrison, 2021; Ocakoğlu et al., 2019b). Likewise, nodal sites like Troy contain multiple fire episodes between cal. 2200–2000 BCE (Ünlüsoy, 2018). Massa (2014) demonstrates that fire events across Central and Western Anatolia reach the first peak around mid-third millennium B.C. and then another peak is reached around cal. 2200 BCE One of the reasons why the timeliness of these fires, abandonments and/or re-organisations may be a result of the arid phase in these centuries, which put political and economic structures under stress and made them extremely vulnerable. Yet again, the lack of archaeological data from the Simav area impedes direct comparison of the lake data with archaeological proxies.

Yet another major arid phase is recognised in the 10-9th centuries B.C. (Early Iron Age) when the annual rainfall is estimated to have fallen below 478 mm (Fig. 10A, Table 3). This period partly coincides and postdates the globally recognised 3.2 ka rapid climate change, marking a widespread political crisis and societal collapse after cal. 1200 BCE in the eastern Mediterranean (Weiss et al., 1993; Kaniewski et al., 2015). However, in this case, the climatic trend of aridity might have lasted much longer than a few generations. Paleoclimatic proxies suggest that there is a long-term cold and arid phase that lasted globally almost until the Roman Climatic Optimum (Drake, 2012). Our results from Lake Simav show an arid episode that lasts until 500 BCE, in line with the global trends.

In Anatolia, the collapse of the Hittite Kingdom and the emergence of new polities afterward are directly associated with a severe drought as a consequence of this arid phase and the 3.2 ka event (Seeher, 2010; Ross et al., 2019). In archaeological terms, the Early Iron Age in western Anatolia is poorly understood and is mainly associated with human mobility and migrations from the Balkans. This movement of people manifested itself in the archaeological record as a new type of architecture and hand-made pottery (Voigt and Henrickson, 2000). These groups established settlements around Ankara, Eskişehir, and Kütahya which evolved into the Phrygian Kingdom with its capital at Gordion (Tüfekçi Sivas, 2007a, 2007b). Recent archaeological work at Gordion shows a continuation of habitation from the 10th into the 4th century B.C without a phase of abandonment (Rose, 2017). Kealhofer and Marsch (2019) suggest that it was possible for Phrygian groups to thrive within this long-term aridity phase by adapting various agro-pastoral strategies such as irrigation farming, caprine management, grazing and pastoralism.

Multi-proxy paleoclimatic data indicates that 200 BCE - 150 CE can be identified as the “Roman Climate Optimum” in the Mediterranean with stable, warm and humid conditions (McCormick et al., 2012). Lake Simav proxies (Fig. 7) demonstrate high lake levels and rainfall was prevalent after 250 BCE which coincides well with the Roman Climate Optimum. Archaeological data from Kütahya is consistent with this picture. Multiple cities were founded in Kütahya Region during the Hellenistic and Roman periods (Ramsay, 1960). Among these, Aizanoi (Çavdarhisar) is archaeologically well researched. During the Imperial period, Aizanoi became prosperous by producing cereals, wool and wine, all pointing towards favorable and stable climatic conditions (Özer, 2011). In this sense, Lake Simav reflects this favorable environment during this period.

9. Conclusion

We traced the Holocene climatic changes in Lake Simav (W Anatolia), which swung between endorheic and exhorheic conditions throughout its history, using a bunch of techniques ranging from sedimentology to hydro-balance modeling. Sedimentological observations coupled with analytical multi-proxy data revealed the precise lake level fluctuations whereas a hydro-balance model based on the modern hydrological dataset enabled the absolute precipitation estimations for some past endorheic periods.

We discovered centennial colluvial wedge developments over lacustrine sediments at around 8.0 ka, 3.8 ka, 2.9 ka, 2.4 ka and 2.0 ka. Our past hydro-balance model results demonstrate that during the formation of the first three wedges that can match with the global dry events of 8.2 ka, 4.2 ka and 3.2 ka, the annual precipitations would have been below 460 mm, 468 mm, and 478 mm respectively, whereas the current precipitation fluctuates around 800 mm. These drought events have contemporaneous correlatives in Eski Acıgöl (Central Anatolia) and Lake Gölhisar (SW Anatolia contemporaneous) records, that indicate climate was a dominant driver on sediment dynamics (Fig. 10). In the Chalcolithic-Early Bronze Age I periods between 4000 and 2000 BCE, the lake level was generally high and the lake was outflowing. Although we lack local archaeological proxies, this was a period of proliferation characterised by the increased number of settlements, the appearance of centralised and fortified places, and the political re-organisations in western Anatolia in general. The 4.2 ka event started

at around 2150 BCE in the Simav area and reached a climax grossly around 1800 BCE with annual precipitation <468 mm. A precipitation deficit of likely more than 20% in this event compared to the previous wet period was coeval with frequent fires and widespread abandonment of Early Bronze Age settlements in wider western and central Anatolia (Massa, 2014). Similarly, a subsequent wet period ($P > 500$ mm) of high lake level was interrupted first by a mild drought at about 1050 BCE (3.2 ka event) and turned out later a severe drought with less than 478 mm annual precipitation at 816 BCE This long-term aridity lasted until ca. 500 BCE in Lake Simav, which is in line with the regional paleoclimatic proxies. The local political entities around this time adapted to aridity by implementing a variety of agro-pastoral and residential strategies which kept them resilient in the face of a long-lasting drought that only ceased with the Roman Climatic Optimum around 250 BCE.

Declaration of Competing Interest

The authors declare that they have no known competing financial interests or personal relationships that could have appeared to influence the work reported in this paper.

Acknowledgments

The authors are grateful to Dr. Fatima Makodem (CNRS) for her help in the fieldwork, and Ayşegül Dikme (ESOGÜ) for her contribution to the laboratory studies. Clay Campbell (University of Kansas) kindly edited the manuscript. This study was financially supported by the Commission for Scientific Research at Eskişehir Osmangazi University, Turkey (Grant number: 2016-15050).

Appendix A. Supplementary data

Supplementary data to this article can be found online at https://doi.org/10.1016/j.palaeo.2022.111001.

References

ALOS PALSAR, 2020. https://doi.org/10.5067/Z97HFCNKR6VA (Accessed 20 March 2020).
Arıkan, B., Yıldırım, T., 2018. Paleoclimate, geology, geomorphology, and Middle Holocene settlement systems in the Delice valley of north-Central Anatolia. J. Field Archaeol. 43 (8), 570–590.
Bar-Matthews, M., Ayalon, A., 2011. Mid-Holocene climate variations revealed by high-resolution speleothem records from Soreq Cave, Israel and their correlation with cultural changes. The Holocene 21 (1), 163–171.
Battarbee, R.W., 1986. Diatom analysis. In: Berglund, B.E. (Ed.), Handbook of Holocene Paleoecology and Paleohydrology. J. Wiley and Sons, London, pp. 527–571.
Bellin, N., Vanacker, V., De Baets, S., 2013. Anthropogenic and climatic impact on Holocene sediment dynamics in SE Spain: a review. Quat. Int. 308, 112–129.
Bingöl, N.A., Korkmaz, M., 2013. 1961 yılından günümüze Simav Gölü (Kütahya). Dumlupınar Üniversitesi Fen Bilimleri Enstitüsü Dergisi 031, 1–12.
Blikra, L.H., Nemec, W., 1998. Postglacial colluvium in western Norway: depositional processes, facies and palaeoclimatic record. Sedimentology 45 (5), 909–960.
Bogaard, A., 2005. 'Garden agriculture' and the nature of early farming in Europe and the near East. World Archaeol. 37 (2), 177–196.
Boggs, S., 1995. Principles of Sedimentology and Stratigraphy, vol. 774. Prentice Hall, New Jersey.
Bond, G., Showers, W., Cheseby, M., Lotti, R., Almasi, P., deMenocal, P., Priore, P., Cullen, H., Hajdas, I., Bonani, G., 1997. A pervasive millennial-scale cycle in North Atlantic Holocene and glacial climates. Science 278 (5341), 1257–1266.
Bookhagen, B., Haselton, K., Trauth, M.H., 2001. Hydrological modelling of a Pleistocene landslide-dammed lake in the Santa Maria Basin, NW Argentina. Palaeogeogr. Palaeoclimatol. Palaeoecol. 169 (1–2), 113–127.
Boussafir, M., Sifeddine, A., Jacob, J., Foudi, M., Cordeiro, R.C., Albuquerque, A.L.S., Turcq, B., 2012. Petrographical and geochemical study of modern lacustrine sedimentary organic matter (Lagoa do Caçò, Maranão, Brazil): Relationship between early diagenesis, organic sedimentation and lacustrine filling. Org. Geochem. 47, 88–98.
Bozkurt, E., 2001. Neotectonics of Turkey-a synopsis. Geodin. Acta 14, 3–30.
Brazier, V., Ballantyne, C.K., 1989. Late Holocene debris cone evolution in Glen Feshie, western Cairngorm Mountains, Scotland. Earth Environ. Sci. Trans. Royal Soc. Edinb. 80 (1), 17–24.
Bryson, R.A., DeWall, K.M., 2007. A Paleoclimatology Workbook: High Resolution, Site-Specific, Macrophysical Climate Modeling. Mammoth Site of Hot Springs, SD Inc, Hot Springs, SD.
Çakırlar, C., 2012a. Evolution of animal husbandry in Neolithic Central-West Anatolia, the archaeozoological record from Ulucak Höyük (ca. 7040-5660 cal. B.C., İzmir, Turkey). Anatol. Stud. 62 (1), 1–33.
Çakırlar, C., 2012b. Neolithic Dairy Technology at the European-Anatolian Frontier: Implications of Archaeozoological evidence from Ulucak Höyük, Izmir, Turkey, ca. 7000-5700 cal. B.C. Anthropozoologica 47 (2), 79–100.
Çakıroğlu, A.İ., Levi, E.E., Tavşanoğlu, Ü.N., Bezirci, G., Erdoğan, Ş., Filiz, N., Andersen, T.J., Davidson, T.A., Jeppesen, E., Beklioğlu, M., 2016. Inferring past environmental changes in three Turkish lakes from sub-fossil Cladocera. Hydrobiologia 778 (1), 295–312.
Christol, A., Kuzucuoğlu, C., Fort, M., Mouralis, D., Doğu, A.F., Akköprü, E., Zorer, H., 2010. Morphosedimentary evidences of lake level variations in the terraces of Lake Van (Turkey). Quaternaire 21 (4), 443–458.
Çilingiroğlu, Ç., Ünlüsoy, S., 2017. Negotiating peace, enduring conflict: a diachronic view on prehistoric warfare in the Eastern Aegean. In: Kozal, E., Akar, M., Heffron, Y., Çilingiroğlu, Ç., Şerifoğlu, T.E., Çakırlar, C., Jean, S. Ünlüsoy Ve E. (Eds.), Questions, Approaches, and Dialogues in Eastern Mediterranean Archaeology Studies in Honor of Marie-Henriette and Charles Gates, Ugarit-Verlag, pp. 97–124.
Collinson, J.D., 1978. Lakes. In: Reading, H.G., Reading, H.G. (Eds.), Sedimentary Environments and Facies, 60. Blackwell, Oxford, pp. 61–79.
Davis, B.A., Brewer, S., Stevenson, A.C., Guiot, J., 2003. The temperature of Europe during the Holocene reconstructed from pollen data. Quat. Sci. Rev. 22 (15–17), 1701–1716.
Dean, W.E., Fouch, T.D., 1983. Carbonate Depositional Environments. The American Association Annexes.
Dean, J.R., Jones, M.D., Leng, M.J., Noble, S.R., Metcalfe, S.E., Sloane, H.J., Shay, D., Eastwood, W.J., Roberts, C.N., 2015. Eastern Mediterranean hydroclimate over the late glacial and Holocene, reconstructed from the sediments of Nar lake, Central Turkey, using stable isotopes and carbonate mineralogy. Quat. Sci. Rev. 124, 162–174.
Degens, E., Kempe, S., Richey, J.E., 1991. Biogeochemistry of Major World Rivers, SCOPE Report 42. John Wiley and Sons, Chichester, p. 356.
Devlet, Su, 2020. İşleri Genel Müdürlüğü. https://www.dsi.gov.tr/Sayfa/Detay/744 (accessed 30 March 2020).
DeVogel, S.B., Magee, J.W., Manley, W.F., Miller, G.H., 2004. A GIS-based reconstruction of late Quaternary paleohydrology: Lake Eyre, arid Central Australia. Palaeogeogr. Palaeoclimatol. Palaeoecol. 204 (1–2), 1–13.
Dieffenbacher-Krall, A.C., Vandergoes, M.J., Denton, G.H., 2007. An inference model for mean summer air temperatures in the Southern Alps, New Zealand, using subfossil chironomids. Quat. Sci. Rev. 26 (19–21), 2487–2504.
Dormoy, I., Peyron, O., Combourieu-Nebout, N., Goring, N.S., Kotthoff, U., Magny, M., Pross, J., 2009. Terrestrial climate variability and seasonality changes in the Mediterranean region between 15 000 and 4000 years BP deduced from marine pollen records. Clim. Past Discuss. 5, 735–770.
Drake, B.L., 2012. The influence of climatic change on the late Bronze Age Collapse and the Greek Dark Ages. J. Archaeol. Sci. 39 (6), 1862–1870.
Dusar, B., Verstraeten, G., Notebaert, B., Bakker, J., 2011. Holocene environmental change and its impact on sediment dynamics in the Eastern Mediterranean. Earth Sci. Rev. 108 (3–4), 137–157.
Dusar, B., Verstraeten, G., D'haen, K., Bakker, J., Kaptijn, E., Waelkens, M., 2012. Sensitivity of the Eastern Mediterranean geomorphic system towards environmental change during the late Holocene: a chronological perspective. J. Quat. Sci. 27 (4), 371–382.
Eastwood, W.J., Leng, M.J., Roberts, N., Davis, B., 2007. Holocene climate change in the eastern Mediterranean region: a comparison of stable isotope and pollen data from Lake Gölhisar, Southwest Turkey. J. Quat. Sci. Publ. Quat. Res. Assoc. 22 (4), 327–341.
Efe, T., 1995. İç Batı Anadolu'da İki Neolitik Yerleşme: Fındık Kayabaşı ve Akmakça. In: Erkanal, H., et al. (Eds.), Memoriam İ. Metin Akyurt-Bahattin Devam Anı Kitabı, İstanbul, Arkeoloji ve Sanat Yayınları, pp. 105–114.
Efe, T., 2007. The theories of the Great Caravan Route between Cilicia and Troy: the early Bronze Age III period in inland western Anatolia. Anatol. Stud. 57, 47–64.
Efe, T., Gatsov, I., and Nedelcheva, P. (2012) "Keçiçayırı. A Neolithic Settlement near Seyitgazi, Eskişehir." The Neolithic in Turkey. New excavations and new research. Volume 4: Western Turkey. M. Özdoğan, N. Başgelen Ve P. Kuniholm (der.), İstanbul: Arkeoloji ve Sanat Yayınları, 227–236.
Emre, Ö., Duman, T.Y., 2011. 19 Mayıs 2011 Simav (Kütahya) Depremi (Mw=5,8) Ön Değerlendirmesi. Jeoloji Etütleri Dairesi İç raporu, MTA Genel Müdürlüğü, p. 5.
England, A., Eastwood, W.J., Roberts, C.N., Turner, R., Haldon, J.F., 2008. Historical landscape change in Cappadocia (Central Turkey): a palaeoecological investigation of annually laminated sediments from Nar lake. The Holocene 18 (8), 1229–1245.
Eriş, K.K., Ön, S.A., Çağatay, M.N., Ülgen, U.B., Ön, Z.B., Gürocak, Z., Arslan, T.N., Akkoca, D.B., Damcı, E., İnceöz, M., Okan, Ö.Ö., 2018. Late Pleistocene to Holocene Paleoenvironmental Evolution of Lake Hazar, Eastern Anatolia, Turkey. Quat. Int. 486, 4–16.
Eser, T., 1997. Eynal-Çitgöl-Naşa (Simav-Kütahya) sıcak ve mineralli sularının hidrojeolojisi. Pamukkale University, Graduate School of Natural and Applied Sciences, p. 122.
Fidan, E., Türkteki, M., Türkteki, S., Oğuzhanoğlu, U., Akay, Seçer Fidan, S. and Tuna, Y., 2020. Eskişehir ve Kütahya illeri tarih öncesi dönem yüzey araştırmaları (EKAR) 2018 yılı çalışmaları. Araştırma Sonuçları Toplantısı 37 (2), 15–34.
Finné, M., Woodbridge, J., Labuhn, I., Roberts, C.N., 2019. Holocene hydro-climatic variability in the Mediterranean: a synthetic multi-proxy reconstruction. The Holocene 29 (5), 847–863.

Frumkin, A., 2009. Stable isotopes of a subfossil Tamarix tree from the Dead Sea region, Israel, and their implications for the Intermediate Bronze Age environmental crisis. Quat. Res. 71 (3), 319–328.
Grillone, G., Baiamonte, G., D'Asaro, F., 2014. Empirical determination of the average annual runoff coefficient in the Mediterranean area. Am. J. Appl. Sci. 11 (1), 89.
Groenhuijzen, M.R., Kluiving, S.J., Gerritsen, F.A., Künzel, M., 2014. Geoarchaeological research at Barcın Höyük: implications for the initial Neolithic occupation of Northwest Anatolia. Quat. Int. 367, 51–61.
Harrison, T.P., 2021. The Iron Age I–II transition in the Northern Levant: an emerging consensus? Jerusalem J. Archaeol. 1, 325–351.
Haslett, J., Parnell, A.C., 2008. A simple monotone process with application to radiocarbon-dated depth chronologies. J. R. Stat. Soc.: Ser. C: Appl. Stat. 57 (4), 399–418.
Hastenrath, S., Kutzbach, J.E., 1983. Paleoclimatic estimates from water and energy budgets of East African lakes. Quat. Res. 19 (2), 141–153.
Heiri, O., Lotter, A.F., Lemcke, G., 2001. Loss on ignition as a method for estimating organic and carbonate content in sediments: reproducibility and comparability of results. J. Paleolimnol. 25 (1), 101–110.
Helfer, F., Lemckert, C., Zhang, H., 2012. Impacts of climate change on temperature and evaporation from a large reservoir in Australia. J. Hydrol. 475, 365–378.
Hoegh-Guldberg, O., Jacob, D., Bindi, M., Brown, S., Camilloni, I., Diedhiou, A., Hijioka, Y., 2018. Impacts of 1.5 C global warming on natural and human systems. In: Global warming of 1.5° C. An IPCC Special Report.
Horejs, B., Galik, A., 2011. Aktivitäten und Subsistenz in den Siedlungen des Çukuriçi Höyük. Der Forschungsstand nach den Ausgrabungen 2006-2009. Praehistorische Zeitschrift 86, 31–66.
Istanbulluoglu, E., Bras, R.L., 2006. On the dynamics of soil moisture, vegetation, and erosion: implications of climate variability and change. Water Resour. Res. 42 (6).
Jalut, G., Dedoubat, J.J., Fontugne, M., Otto, T., 2009. Holocene circum-Mediterranean vegetation changes: climate forcing and human impact. Quat. Int. 200, 4–18.
Jones, P.D., Mann, M.E., 2004. Climate over past millennia. Rev. Geophys. 42 (2).
Jones, M.D., Roberts, C.N., Leng, M.J., Türkeş, M., 2006. A high-resolution late Holocene lake isotope record from Turkey and links to North Atlantic and monsoon climate. Geology 34 (5), 361–364.
Jones, M.D., Roberts, C.N., Leng, M.J., 2007. Quantifying climatic change through the last glacial–interglacial transition based on lake isotope palaeohydrology from Central Turkey. Quat. Res. 67 (3), 463–473.
Jones, P.D., Briffa, K.R., Osborn, T.J., Lough, J.M., van Ommen, T.D., Vinther, B.M., Schmidt, G.A., 2009. High-resolution palaeoclimatology of the last millennium: a review of current status and future prospects. The Holocene 19 (1), 3–49.
Ju, J., Zhu, L.P., Wang, J., Xie, M., Zhen, X., Wang, Y., Peng, P., 2010. Water and sediment chemistry of Lake Pumayum Co, South Tibet, China: implications for interpreting sediment carbonate. J. Paleolimnol. 43 (3), 463–474.
Junginger, A., Trauth, M.H., 2013. Hydrological constraints of paleo-Lake Suguta in the Northern Kenya Rift during the African humid period (15–5 ka BP). Glob. Planet. Chang. 111, 174–188.
Kaniewski, D., Paulissen, E., De Laet, V., Dossche, K., Waelkens, M., 2007. A high-resolution late Holocene landscape ecological history inferred from an intramontane basin in the Western Taurus Mountains, Turkey. Quat. Sci. Rev. 26 (17–18), 2201–2218.
Kaniewski, D., Guiot, J., Van Campo, E., 2015. Drought and societal collapse 3200 years ago in the Eastern Mediterranean: a review. WIREs Clim. Change 6, 369–382. https://doi.org/10.1002/wcc.345.
Kaniewski, D., Marriner, N., Cheddadi, R., Guiot, J., Van Campo, E., 2018. The 4.2 kaBP event in the Levant. Clim. Past 14, 1529–1542.
Kealhofer, L., Marsch, B., 2019. Agricultural impact and political economy: Niche construction in the Gordion region, Central Anatolia. Quat. Int. 529, 91–99.
Koçyiğit, A., Deveci, S., 2005. Aksehir-Simav fault system: commencement age of neotectonic regime and seismicity. SW Turkey. In: 2005 earthquake symposium, Kocaeli (in Turkish) symposium, Kocaeli (in Turkish).
Kohfeld, K.E., Harrison, S.P., 2000. How well can we simulate past climates? Evaluating the models using global palaeoenvironmental datasets. Quat. Sci. Rev. 19 (1–5), 321–346.
Küçük, M., Kahya, E., Cengiz, T.M., Karaca, M., 2009. North Atlantic oscillation influences on Turkish lake levels. Hydrol. Proc. Int. J. 23 (6), 893–906.
Kukla, G., Heller, F., Ming, L.X., Chun, X.T., Sheng, L.T., Sheng, A.Z., 1988. Pleistocene climates in China dated by magnetic susceptibility. Geology 16 (9), 811–814.
Kutzbach, J.E., Guetter, P.J., 1986. The influence of changing orbital parameters and surface boundary conditions on climate simulations for the past 18 000 years. J. Atmos. Sci. 43 (16), 1726–1759.
Kutzbach, J.E., Guetter, P.J., Behling, P.J., Selin, R., 1993. Simulated climatic changes: results of the COHMAP climate-model experiments. In: Global Climates Since the Last Glacial Maximum, pp. 24–93.
Kuzucuoğlu, C., 2002. Environmental setting and evolution from the 9th to the 5th millennium cal B.C. in Central Anatolia: An introduction to the study of relations between environmental conditions and the development of human societies. In: The Neolithic of Central Anatolia, Internal Developments and External Relations during the 9th–6th Millennia cal B.C, pp. 33–58.
Kuzucuoğlu, C., Christol, A., Mouralis, D., Doğu, A.F., Akköprü, E., Fort, M., Scaillet, S., 2010. Formation of the upper pleistocene terraces of Lake Van (Turkey). J. Quat. Sci. 25 (7), 1124–1137.
Kuzucuoğlu, C., Dörfler, W., Kunesch, S., Goupille, F., 2011. Mid- to late-Holocene climate change in Central Turkey: the Tecer Lake record. The Holocene 21 (1), 173–188.
Lacey, J.H., Jones, M.D., 2018. Quantitative reconstruction of early Holocene and last glacial climate on the Balkan Peninsula using coupled hydrological and isotope mass balance modelling. Quat. Sci. Rev. 202, 109–121.
Laird, K.R., Cumming, B.F., 2008. Reconstruction of Holocene lake level from diatoms, chrysophytes and organic matter in a drainage lake from the Experimental Lakes Area (northwestern Ontario, Canada). Quat. Res. 69 (2), 292–305.
Landmann, G., Reimer, A., Kempe, S., 1996. Climatically induced lake level changes at Lake Van, Turkey, during the Pleistocene/Holocene transition. Glob. Biogeochem. Cycles 10 (4), 797–808.
Lavee, H., Imeson, A.C., Sarah, P., 1998. The impact of climate change on geomorphology and desertification along a Mediterranean-arid transect. Land Degrad. Dev. 9 (5), 407–422.
Leng, M.J., Lamb, A.L., Heaton, T.H., Marshall, J.D., Wolfe, B.B., Jones, M.D., et al., 2006. Isotopes in lake sediments. In: Isotopes in Palaeoenvironmental Research. Springer, Dordrecht, pp. 147–184.
Lionello, P., Malanotte-Rizzoli, P., Boscolo, R., Luterbacher, J., 2004. The Mediterranean Climate: Basic Issues and Perspectives. White Paper on Mediterranean climate variability and predictability, Technical Report, pp. 5–17.
Maher, B.A., Thompson, R., 1991. Mineral magnetic record of the Chinese loess and paleosols. Geology 19 (1), 3–6.
Mann, M.E., 2002. Little ice age. Encyclop. Glob. Environ. Change 1, 504–509.
Marino, G., Rohling, E.J., Sangiorgi, F., Hayes, A., Casford, J.L., Lotter, A.F., et al., 2009. Early and middle Holocene in the Aegean Sea: interplay between high and low latitude climate variability. Quat. Sci. Rev. 28 (27–28), 3246–3262.
Marston, J.M., Çakırlar, C., Luke, C., Kováčik, P., Slim, F.G., Shin, N., Roosevelt, C.H., 2021. Agropastoral Economies and Land Use in Bronze Age Western Anatolia. Environ. Archaeol. https://doi.org/10.1080/14614103.2021.1918485.
Massa, M., 2014. Destructions, abandonment, social reorganisation and climatic change in west and Central Anatolia at the end of the third millennium B.C. In: Erciyas, B., Sökmen, E. (Eds.), Arkeolojide Bölgesel Çalışmalar Sempozyum Bildirileri, YAS, vol. 4, pp. 89–123.
Massa, M., Şahoğlu, V., 2015. The 4.2 ka Climatic Event in west and Central Anatolia: Combining Palaeoclimatic Proxies and Archaeological Data. H. Meller, R. Risch, R. Jung, RW Arz (eds), 2200, pp. 61–78.
Mayewski, P.A., Rohling, E.E., Stager, J.C., Karlén, W., Maasch, K.A., Meeker, L.D., Meyerson, E.A., Gasse, F., van Kreveld, S., Holmgren, K., Lee-Thorp, J., Rosqvist, G., Rack, F., Staubwasser, M., Schneider, R.R., Steig, E.J., 2004. Holocene climate variability. Quat. Res. 62 (3), 243–255.
McCormick, M., Büntgen, U., Cane, M., Cook, E.R., Harper, K., Huybers, P., Litt, T., Manning, S.W., Mayewski, P.A., More, A.F.M., Nicolussi, K., Tegel, W., 2012. Climate change during and after the Roman Empire: reconstructing the past from scientific and historical evidence. J. Interdiscip. Hist. 43 (2), 169–220.
Meschis, M., Roberts, G.P., Mildon, Z.K., Robertson, J., Michetti, A.M., Faure Walker, J. P., 2019. Slip on a mapped normal fault for the 28th December 1908 Messina earthquake (Mw 7.1) in Italy. Sci. Rep. 9 (1), 1–8.
Meteoroloji Genel Müdürlüğü, 2020. https://mevbis.mgm.gov.tr/mevbis/ui/index.html#/ (accessed with special permission 15 March 2020).
Meyers, P.A., Teranes, J.L., 2001. Sediment Organic Matter, Tracking Environmental Change Using Lake Sediments, Physical and Geochemical Methods.
Morecroft, M.D., Keith, S.A., 2009. Plant ecology as an indicator of climate and global change. In: Climate Change. Elsevier, pp. 297–305.
Morrill, C., Meador, E., Livneh, B., Liefert, D.T., Shuman, B.N., 2019. Quantitative model-data comparison of mid-Holocene lake-level change in the central Rocky Mountains. Clim. Dyn. 53 (1–2), 1077–1094.
MTA, 2002. 1/500.000 ölçekli Türkiye Jeoloji Haritası, İzmir Paftası.
Mullins, C.E., 1977. Magnetic susceptibility of the soil and its significance in soil science–a review. J. Soil Sci. 28 (2), 223–246.
Nemec, W., Kazancı, N., 1999. Quaternary colluvium in west-Central Anatolia: sedimentary facies and palaeoclimatic significance. Sedimentology 46 (1), 139–170.
Ocakoğlu, F., Akbulut, A., Tunoğlu, C., Akkiraz, S., Aşkım Gümüş, B., Görüm, T., Tün, T., Pekkan, E., 2019a. Morphotectonic and palaeoclimatological Investigation of the Simav Graben (Kütahya, W Anatolia). In: Eskişehir Osmangazi University Research Project, Proje no: 2016/15050, Final Project Report, p. 88.
Ocakoğlu, F., Çilingiroğlu, Ç., Erkara, İ.P., Ünan, S., Dinçer, B., Akkiraz, M.S., 2019b. Human-climate interactions since the neolithic period in Central Anatolia: Novel multi-proxy data from the Kureyşler area, Kütahya, Turkey. Quat. Sci. Rev. 213, 1–17.
Owen, J.J., Amundson, R., Dietrich, W.E., Nishiizumi, K., Sutter, B., Chong, G., 2011. The sensitivity of hillslope bedrock erosion to precipitation. Earth Surf. Process. Landf. 36 (1), 117–135.
Oybak-Dönmez, E., Ocakoğlu, F., Akbulut, A., Tunoğlu, C., Gümüş, B.A., Tuncer, A., Görüm, T., Tün, M., 2021. Vegetation record of the last three millennia in Central Anatolia: archaeological and palaeoclimatic insights from Mogan Lake (Ankara, Turkey). Quat. Sci. Rev. 262, 106973.
Özden, S., Tutkun, G.Z.C., Bekler, T., Karaca, Ö., Komut, T., Kalafat, D., Ateş, Ö., Demirci, A., Gündoğdu, E., Çınar, S., 2012. Simav Fayı ile Kütahya Fayı (Emet-Orta Batı Anadolu) arasında kalan bölgenin Neotektonik ve sismotektonik özellikleri. In: TÜBİTAK ÇAYDAG proje no: 109Y103, p. 212.
Özer, E., 2011. İçinden Su Geçen Şehir: Aizanoi. Toplumsal Tarih 215, 90–93.
Parnell, A.C., Haslett, J., Allen, J.R.M., Buck, C.E., Huntley, B., 2008. A flexible approach to assessing synchroneity of past events using Bayesian reconstructions of sedimentation history. Quat. Sci. Rev. 27 (19–20), 1872–1885.
Polissar, P.J., Abbott, M.B., Shemesh, A., Wolfe, A.P., Bradley, R.S., 2006. Holocene hydrologic balance of tropical South America from oxygen isotopes of lake sediment opal, Venezuelan Andes. Earth Planet. Sci. Lett. 242 (3–4), 375–389.

Pribyl, P., Shuman, B.N., 2014. A computational approach to Quaternary lake-level reconstruction applied in the central Rocky Mountains, Wyoming, USA. Quat. Res. 82 (1), 249–259.
Pross, J., Kotthoff, U., Müller, U.C., Peyron, O., Dormoy, I., Schmiedl, G., Smith, A.M., 2009. Massive perturbation in terrestrial ecosystems of the Eastern Mediterranean region associated with the 8.2 kyr BP climatic event. Geology 37 (10), 887–890.
Quezel, P., Barbero, M., 1985. Carte de la végétation potentielle de la région méditerranéenne, feuille 1. Mediterranée orientate.
Ramsay, W.M., 1960. Anadolu'nun Tarihi Coğrafyası.Mihri Pektaş (çev.). Milli Eğitim Basımevi, İstanbul.
Recep, E.F.E., 1998. Yukarı Gediz havzasında iklimin doğal bitki örtüsü dağılışına etkisi. Türk Coğrafya Dergisi 33, 79–99.
Reineck, H.E., Singh, I.B., 1980. Depositional environments. In: Depositional Sedimentary Environments. Springer, Berlin, Heidelberg, pp. 5–7.
Reyer, C.P., Otto, I.M., Adams, S., Albrecht, T., Baarsch, F., Cartsburg, M., Mengel, M., 2017. Climate change impacts in Central Asia and their implications for development. Reg. Environ. Chang. 17 (6), 1639–1650.
Richardson, P.W., Perron, J.T., Schurr, N.D., 2019. Influences of climate and life on hillslope sediment transport. Geology 47 (5), 423–426.
Riebe, C.S., Kirchner, J.W., Finkel, R.C., 2004. Erosional and climatic effects on long-term chemical weathering rates in granitic landscapes spanning diverse climate regimes. Earth Planet. Sci. Lett. 224 (3–4), 547–562.
Roberts, N., Reed, J.M., Leng, M.J., Kuzucuoğlu, C., Fontugne, M., Bertaux, J., Karabiyikoğlu, M., 2001. The tempo of Holocene climatic change in the eastern Mediterranean region: new high-resolution crater-lake sediment data from Central Turkey. The Holocene 11 (6), 721–736.
Roberts, N., Woodbridge, J., Bevan, A., Palmisano, A., Shennan, S., Asouti, E., 2018. Human responses and non-responses to climatic variations during the last Glacial-Interglacial transition in the eastern Mediterranean. Quat. Sci. Rev. 184, 47–67.
Roberts, C.N., Woodbridge, J., Palmisano, A., Bevan, A., Fyfe, R., Shennan, S., 2019. Mediterranean landscape change during the Holocene: synthesis, comparison and regional trends in population, land cover and climate. The Holocene 29 (5), 923–937.
Rodewald-Rudescu, L., 1974. Das Schilfrohr (*Phragmites communis* Trinius). *Die Binnengewässer*. Band 27, 302. ISBN 978-3-510-40038-6.
Rose, B., 2017. Fieldwork at phyrgian gordion, 2013–2015. Am. J. Archaeol. 121 (1), 135–178.
Ross, J.C., Steadman, S.R., McMahon, G., Adcock, S.E., Cannon, J.W., 2019. When the Giant Falls: Endurance and Adaptation at Çadır Höyük in the Context of the Hittite Empire and its Collapse. J. Field Archaeol. 44 (1), 19–39. https://doi.org/10.1080/00934690.2018.1558906.
Round, F.E., Crawford, R.M., Mann, D.G., 1990. The Diatoms, Biology and Morphology of the Genera. Cambridge University Press, England, p. 747.
Şahin, S., 2012. An aridity index defined by precipitation and specific humidity. J. Hydrol. 444, 199–208.
Şahoğlu, V., 2005. The anatolian trade network and the Izmir Region during the early Bronze Age. Oxf. J. Archaeol. 24 (4), 339–361.
Saldık, S., 2019. Simav Ve Tavşanlı'nın Iklim özellikleri. MSc Thesis. Marmara University, Turkey.
Santisteban, J.I., Mediavilla, R., Lopez-Pamo, E., Dabrio, C.J., Zapata, M.B.R., García, M. J.G., Castaño, S., Martínez-Alfaro, P.E., 2004. Loss on ignition: a qualitative or quantitative method for organic matter and carbonate mineral content in sediments. J. Paleolimnol. 32 (3), 287–299.
Sariş, F., Hannah, D.M., Eastwood, W.J., 2010. Spatial variability of precipitation regimes over Turkey. Hydrol. Sci. J. J. Sci. Hydrol. 55 (2), 234–249.
Schwall, C., Horejs, B., 2020. Social dynamics in Western Anatolia between 3000 and 2500 B.C. In: Blum, W.E., Efe, T., Kienlin, T.L., Pernicka, E. (Eds.), From Past to Present. Studies in Memory of Manfred O. Korfmann, Studia Troica Monographien, 11, pp. 109–119 (Bonn 2020).
Seeher, J., 2010. After the Empire: observations on the early iron age in Central Anatolia. In: Singer, I. (Ed.), Ipamati Kistamati Pari Tumatimis: Luwian and Hittite Studies Presented to J. David Hawkins on the Occasion of his70th Birthday. Tel Aviv University, Tel Aviv, pp. 220–229.
Sicim, E., 2010. Simav Gölü'nün Kurutulmasının Yarattığı Değişimler, Yüksek Lisans Tezi, İstanbul Üniversitesi, Sosyal Bilimler Enstitüsü, İstanbul.
Simav Ticaret ve Sanayi Odası, 2020. https://www.simavtso.org.tr/ (Accessed 15 March 2020).
Stan, F.I., Neculau, G., Zaharia, L., Ioana-Toroimac, G., Mihalache, S., 2016. Study on the evaporation and evapotranspiration measured on the Căldăruşani Lake (Romania). Proc. Environ. Sci. 32, 281–289.
Staubwasser, M., Weiss, H., 2006. Holocene climate and cultural evolution in late prehistoric-early historic West Asia. Quat. Res. 66, 372–387.
Stuiver, M., Reimer, P.J., Reimer, R.W., 2021. CALIB 8.2 [WWW program]. at. http://calib.org. Accessed 2021-01-05.
Talbot, M.R., 2004. Nitrogen isotopes in palaeoclimatology. In: Smol, J.P., Smol, J.P., Birks, H.J.B., Last, W.M. (Eds.), Tracking environmental change using lake sediments, Volume 2: Physical and Geochemical Methods. Kluwer Academic Publishers, Dordrecht, The Netherlands, pp. 401–439.
Tatlı, H., Nüzhet Dalfes, H., Sibel Menteş, Ş., 2004. A statistical downscaling method for monthly total precipitation over Turkey. Int. J. Climatol. J. Royal Meteorol. Soc. 24 (2), 161–180.
Tóth, M., Magyari, E.K., Buczkó, K., Braun, M., Panagiotopoulos, K., Heiri, O., 2015. Chironomid-inferred Holocene temperature changes in the South Carpathians (Romania). The Holocene 25 (4), 569–582.
Touchan, R., Akkemik, Ü., Hughes, M.K., Erkan, N., 2007. May–June precipitation reconstruction of southwestern Anatolia, Turkey during the last 900 years from tree rings. Quat. Res. 68 (2), 196–202.
Tüfekçi Sivas, T. (2007a). Frigler ve Frig Uygarlığı. Friglerin Gizemli Uygarlığı. H. Sivas Ve, T. Tüfekçi Sivas (der.), Yapı Kredi Kültür Sanat Yayıncılık. İstanbul. 9-14.
Tüfekçi Sivas, T. (2007b). Batı Frigya'da Frig Yerleşmeleri ve Kaya Anıtlarının Araştırılması", Friglerin Gizemli Uygarlığı. H. Sivas Ve, T. Tüfekçi Sivas (der.), Yapı Kredi Kültür Sanat Yayıncılık. İstanbul. 77-92.
Türkeş, M., Erlat, E., 2003. Precipitation changes and variability in Turkey linked to the North Atlantic Oscillation during the period 1930–2000. Int. J. Climatol. J. Royal Meteorol. Soc. 23 (14), 1771–1796.
Türktüzün, M., Ünan, S., Ünal, S., 2014. Çiledir Höyük Erken Tunç Çağı II Bulguları. TÜBA-AR 17, 49–72.
Türktüzün, M., Ünan, N., Inal, S., 2015a. Höyüktepe 2014 Yılı Erken Tunç Çağı Metal Bulgularına Dair Bir Değerlendirme. In: Türktüzün, M., Ünan, S. (Eds.), Kureyşler Barajı Kurtarma Kazıları 2014. Bilgin Kültür Yayınevi, Ankara, pp. 473–486.
Türktüzün, M., Ünan, S., Ünan, N., Bilgiç, H., 2015b. Kureyşler Barajı Kurtarma Kazıları 2014 Yılı Çalışmaları. In: Müze Kurtarma Kazıları Sempozyumu ve 1. Uluslararası Müzecilik Çalıştayı, 24, pp. 469–478.
Ülgen, U.B., Franz, S.O., Biltekin, D., Çağatay, M.N., Roeser, P.A., Doner, L., Thein, J., 2012. Climatic and environmental evolution of Lake Iznik (NW Turkey) over the last ~4700 years. Quat. Int. 274, 88–101.
Ünal, Y., Kindap, T., Karaca, M., 2003. Redefining the climate zones of Turkey using cluster analysis. Int. J. Climatol. J. Royal Meteorol. Soc. 23 (9), 1045–1055.
Ünlüsoy, S., 2018. Social Change during the early Bronze Age in Western Anatolia. Cedrus VI 105–124.
Vermoere, M., Smets, E., Waelkens, M., Vanhaverbeke, H., Librecht, I., Paulissen, E., Vanhecke, L., 2000. Late holocene environmental change and the record of human impact at gravgaz near sagalassos, Southwest Turkey. J. Archaeol. Sci. 27, 571–595.
Voigt, M.M., Henrickson, R.C., 2000. Formation of the phrygian state: the early iron age at Gordion. Anatol. Stud. 50, 37–54.
Walling, D.E., 2006. Human impact on land–ocean sediment transfer by the world's rivers. Geomorphology 79 (3–4), 192–216.
Wang, L., Mackay, A.W., Leng, M.J., Rioual, P., Panizzo, V.N., Lu, H., Kendrick, C.P., 2013. Influence of the ratio of planktonic to benthic diatoms on lacustrine organic matter δ13C from Erlongwan maar lake, Northeast China. Org. Geochem. 54, 62–68.
Weiss, H., 2017. 4.2 ka BP Megadrought and the Akkadian Collapse. In: Weiss, H. (Ed.), Megadrought and Collapse. From Early Agriculture to Angkor. Oxford University Press, New York, pp. 93–160.
Weiss, H., Courty, M.A., Wetterstrom, W., Guichard, F., Senio, L., Meadow, R., Curnow, A., 1993. The genesis and collapse of 3rd millenium north Mesopotamian civilization. Science 261, 995–1004.
Wolin, J.A., Duthie, H.C., 1999. Diatoms as indicators of water level change in freshwater lakes. In: Stoermer, E.F., Smol, J.P. (Eds.), The Diatoms: Applications for Environmental and Earth Sciences. Cambridge University Press, Cambridge, pp. 183–202.
Wolin, J.A., Stone, J.R., 2010. Diatoms as indicators of water-level change in freshwater lakes. In: The Diatoms: Applications for the Environmental and Earth Sciences, p. 17.
Woodbridge, J., Roberts, N., 2011. Late Holocene climate of the Eastern Mediterranean inferred from diatom analysis of annually-laminated lake sediments. Quat. Sci. Rev. 30 (23–24), 3381–3392.
Yaltırak, C., 2002. Tectonic evolution of the Marmara Sea and its surroundings. Mar. Geol. 190, 493–529.
Yılmaz, M.A., 2020. İç Batı Anadolu Neolitik-Kalkolitiğine Dair Yeni Bulgular: Düzkışla Höyük, Uşak. Anadolu Araştırmaları 23, 1–40.
Zheng, Y., Zhou, W., Meyers, P.A., Xie, S., 2007. Lipid biomarkers in the Zoigê-Hongyuan peat deposit: Indicators of Holocene climate changes in West China. Org. Geochem. 38 (11), 1927–1940.